Fundamental Continuous-Pulp-Digester Model for Simulation and Control

Philip A. Wisnewski and Francis J. Doyle, III
School of Chemical Engineering, Purdue University, West Lafayette, IN 47907

Ferhan Kayihan
IETek, 5533 Beverly Ave. N.E., Tacoma, WA 98422

A model of a continuous digester was developed as an extension of the well-known Purdue model. A lumped-parameter approximation is used to describe the flow transport mechanism of the digester, and a model based on the fundamental principles of mass and energy is derived. Mass bases and volume fractions are defined to allow fewer simplifying assumptions in the model derivation than in previous model versions. The steady-state profiles and dynamic responses of the digester model are compared with a previous version of the Purdue model, and the significant differences between the two models are highlighted. The digester model is also compared to the Weyerhaeuser benchmark digester model, and a parametric sensitivity analysis to several model parameters is performed. Physical explanations are given for the demonstrated model behaviors. Model implementation is straightforward, making it useful for process control, optimization and design studies.

Introduction

The continuous digester is a tubular reactor in which wood chips react with an aqueous solution of sodium hydroxide and sodium sulfide, referred to as white liquor, to remove the lignin from the cellulose fibers. The product of the digesting process is cellulose fibers, or pulp, which is used to make paper products. Most continuous digesters consist of three basic zones: an impregnation zone, one or more cooking zones, and a wash zone. The white liquor penetrates and diffuses into the wood chips as they flow through the impregnation zone. The white liquor and wood chips are then heated to reaction temperatures and the lignin is removed through one or more cook zones. The free liquor is in either (1) cocurrent or (2) countercurrent flow with respect to the wood chips in the cooking zones. This is where the majority of the delignification reactions occur. The wash zone is the end of the digester where a countercurrent flow of free liquor washes the degradation products from the pulp. This flow also cools the pulp so as to quench the reaction and reduce damage to the cellulose fibers from continued reaction. The Kappa # (number) is a measure of the residual lignin in the pulp and is a direct indicator of pulp quality. The objective is to produce pulp of uniform quality by minimizing variation in the Kappa # from a target value.

This article presents a model for the continuous digester that is derived from the fundamental principles of mass and energy balances. The approach taken for model derivation makes its implementation straightforward. The foundation of the model is a repeating set of ordinary differential equations (ODEs) that can be easily incorporated in simulation packages such as Simulink. The digester is a challenging unit operation for control studies due to unmeasured disturbances, long time delays, nonlinear behavior, and infrequent availability of the control variable measurements. The goal of this work is to provide researchers and practitioners with an easy-to-implement, fundamental continuous digester model that captures the essential dynamic behavior of the digester.

The kraft pulping process for both batch and continuous digesters has been modeled to various levels of complexity. Empirical models for batch digesters using the well-known "H" factor include Vroom (1957) and Hatton (1973, 1976).

Correspondence concerning this article should be addressed to F. J. Doyle, III.
Present address of: P. A. Wisnewski, Weyerhaeuser Company, Technology Center, Tacoma, WA 98477; F. J. Doyle, III, Department of Chemical Engineering, University of Delaware, Newark, DE 19716.

Physically based batch-digester models have been presented in Olm and Tistad (1979), Paulonis and Krishnagopalan (1988), Lee and Datta (1994), and Vanchinathan and Krishnagopalan (1997). The effects of liquor penetration, diffusion, and chip size on the reaction kinetics in kraft pulping have been examined in detail by Gustafson et al. (1983), Jiménez et al. (1989), and Agarwal and Gustafson (1997).

A major effort in the modeling of continuous digesters was initiated by Smith and Williams (1974); the digester model later became known as the Purdue model. In their work, the digester was approximated by a series of continuous stirred-tank reactors (CSTRs) with external flows entering and exiting those CSTRs where the heaters and extraction screens were located. Each CSTR was assumed to contain three phases: a solid phase, which was the wood substance; an entrapped liquor phase, which was the liquor that resided in the pores of the wood chips; and a free-liquor phase, which was the bulk liquor surrounding the wood chips. From chemical pulping data presented in the literature, the kinetic parameters ($A_{i,j}$, $E_{i,j}$, a, b, c) of the pulping reactions were determined (through iterative trials) for the following kinetic model:

$$R_{s,i} = -(k_{1,i}(T)C_{\mathrm{OH}}^{a} + k_{z,i}(T)C_{\mathrm{OH}}^{b}C_{\mathrm{HS}}^{c})(C_{s,i} - C_{s,i}^{\infty}) \quad (1)$$

$$k_{i,j}(T) = A_{i,j}\exp\left(\frac{-E_{i,j}}{RT_c}\right) \qquad i = 1, \ldots, 5 \quad j = 1, 2. \quad (2)$$

The major contribution of their work was the development of the framework in which the digester model would exist and continue to be improved.

Christensen et al. (1982) made a series of modifications that improved the Purdue model. Using additional experimental pulping information, a search algorithm was employed to find the best (least-squares) kinetic parameters for a broader range of wood species. The wood species were divided into hardwood and softwood, and a rate multiplier was used to adjust the kinetics for the different species. Other improvements to the Purdue model were the determination of better lignin ratios, the inclusion of unreactive concentrations of some carbohydrates, improved methods for calculation of reactant consumption, and the incorporation of experimental mass-transfer data. The improved model was found to predict the reactant concentrations in the free liquor at various locations along the digester and the blow-line Kappa # for an industrial digester, even during hardwood/softwood swings.

Considering fluid dynamics in the digester, Härkonen (1987) developed a model from momentum, mass, and energy balances to describe the motion of the chip plug and the bulk liquor. An experimental apparatus that compressed and cooked wood chips was used to develop correlations for the chip compaction and the flow resistance of the free liquor due to compaction. From the experiments, it was also determined that the "volume of wood chip particles remains practically unchanged" during the compression experiments. The resulting model is a set of two-dimensional partial differential equations (PDEs) that are solved at steady state to find velocity (wood chip and liquor), chip pressure, compaction, and temperature profiles along the digester.

Michelsen (1995) combines and extends the work of Härkonen and Christensen to develop a detailed digester model from mass, momentum, and energy balances. His model assumes radial uniformity and rotational symmetry. Like the Purdue model, it is assumed that there are three phases in the digester: solid wood mass, entrapped liquor, and free liquor. In addition to mass components and temperatures, the chip compaction and the wood chip and free-liquor velocities are modeled as well. The physics throughout the digester are described with a complex set of correlations, algebraic equations, ODEs, and PDEs. The model is rescaled using characteristic quantities to reduce numerical stiffness, and is then solved numerically using a staggered grid finite difference method. The model is then used for steady-state and dynamic simulations, linear controllability analysis, model reduction, and proportional-integral control of the wood-chip residence time. The model describes the flow dynamics in detail, but simplifications are made in describing the reaction kinetics. This study suggested that active residence time control by the chip level could yield improved Kappa # control. The model is useful for predicting the effects of flow on the Kappa #; however, the simplification in the kinetics make the model only valid for Kappa # in the range between 50 and 150.

The latest published contribution in continuous digester modeling is by Kayihan et al. (1996). They present a tractable process model that captures the major dynamic characteristics of a continuous digester and offer it to the control research community as a basis to compare contributions and generate interest in digester control studies. Their digester is modeled as a two-vessel Kamyr digester with an impregnation vessel and a reaction vessel. The impregnation zone is modeled as a small mixing zone, followed by a plug-flow zone (pure time delay). The reaction vessel consists of a cocurrent cook zone, a countercurrent modified continuous cook (mcc) zone, and a countercurrent extended modified continuous cook (emcc) zone. The model assumes two phases (nonporous solid and free liquor) in thermal equilibrium, which are modeled with a relatively simple set of PDEs in each zone. The kinetic model of Christensen (1982) is used to describe the reaction of solid material with the liquor phase. There are no diffusion limitations and the heats of reaction are ignored. The set of PDEs is discretized spatially and the model is solved as a set of ODEs. The dynamic characteristics of this benchmark digester model are compared to a proprietary fundamental digester model developed by the Weyerhaeuser Company. The dynamic behavior of the Kappa # to various inputs is captured by the simplified benchmark digester model (Kayihan et al., 1996).

The continuous digester model developed in this article is an extension of the Purdue model, which is an already sound and industrially accepted digester model. Through improved definitions of mass concentrations and volume fractions and a more detailed description of the mass and energy transport within the CSTR, some assumptions necessary in earlier Purdue model versions are removed. The model's ability to extrapolate over wider operating conditions would be expected due to these refinements in model fidelity. The extended Purdue model is compared to the original Purdue model (Butler and Williams, 1988) and the Weyerhaeuser benchmark model (Kayihan et al., 1996). By comparison, it is shown

that the extended Purdue model captures the range of behaviors displayed by these models. The results of these comparisons and discussion of the observed behaviors are given in the Results section. Discussion of possible model uses are included in the Conclusions section.

Model Derivation

The continuous digester is a tubular reactor in which concentration and temperature vary temporally and spatially, characteristic of a distributed parameter system. In this work, a lumped approximation is employed in which a series of CSTRs is used to approximate the axial transport mechanism. Each CSTR is assumed to contain three phases: a solid phase, an entrapped-liquor phase, and a free-liquor phase. Mass and energy balances are calculated for each phase in the CSTR. The resultant set of nonlinear ODEs can be solved numerically with modest computational effort.

The nonlinear ODEs in each CSTR are coupled with those of the neighboring CSTRs through the exchange of state information for each phase in the direction of flow. For instance, wood chips, which consist of the solid and the entrapped-liquor phases, always flow from the top to the bottom of the digester. The solid and entrapped-liquor states for the kth CSTR are the entering solid and entrapped-liquor states for the $k+1$ CSTR. Likewise, in countercurrent flow, the free-liquor states for the kth CSTR are the entering free-liquor states for the $k-1$ CSTR. The external flows from heaters and extraction screens are modeled as flows entering and/or leaving the CSTR. The states and flow rates of the free-liquor phase are adjusted accordingly to account for these external flows.

In a continuous digester, it is expected that thermal and chemical gradients in the radial direction would occur, especially near the heater outlets and extraction screens. By approximating the digester as a series of CSTRs, these gradients as well as wall, entrance, exit, and cross-flow effects are neglected. As the number of CSTRs is increased, the approximation approaches the behavior of a true plug-flow system. However, the size of the lumped-parameter model also increases. Therefore, the number of CSTRs is chosen to trade off model accuracy against computational effort.

Volume fraction definitions

Each CSTR is divided into two volumes, the volume occupied by the wood chips and the volume occupied by the free liquor. The wood chips are assumed to be incompressible, but are compactable. That is, under the weight of the chip column, the individual wood chips maintain their external dimensions, but can be packed closer together. The compaction of chips increases the wood-chip volume and decreases the free-liquor volume in the CSTR. This assumption is supported by the experimental findings of Härkonen (1987). In this work, η will be used to define the ratio of the free-liquor volume to the total CSTR volume. The volume fraction of the free liquor and the wood chips are, respectively:

$$\eta = \frac{\text{volume of free liquor}}{\text{volume of CSTR}}\left[\frac{V_f}{V}\right]$$

$$(1-\eta) = \frac{\text{volume of chip}}{\text{volume of CSTR}}\left[\frac{V_c}{V}\right].$$

The compaction profile of the chips can be modeled empirically as a function of wood chip and liquor flow rates or set to experimentally determined values (Härkonen, 1987). In this study, the compaction profile is assumed to be known and constant with respect to time.

The wood chips are also divided into two volumes, the volume occupied by the solid wood substance and the volume occupied by the entrapped liquor. The entrapped liquor resides in the pores of the wood chips. The porosity, ϵ, is defined to be the volume fraction of the wood chip that is occupied by the entrapped liquor:

$$\epsilon = \frac{\text{volume of entrapped liquor}}{\text{volume of chip}}\left[\frac{V_e}{V_c}\right]$$

$$(1-\epsilon) = \frac{\text{volume of solid}}{\text{volume of chip}}\left[\frac{V_s}{V_c}\right].$$

The porosity of the wood chips changes as a function of the extent of reaction.

Solid-phase component balance

The solid phase comprises the total solid material in the wood chips. It is assumed that all extractive materials, such as the turpenes and resin acids, are removed before the wood chips enter the digester. The solid material is assumed to be homogeneous and to consist of five components: high-reactivity lignin (s_1); low-reactivity lignin (s_2); cellulose (s_3); araboxylan (s_4); and galactoglucomman (s_5). These are the same assumptions for the solid phase used in the earlier versions of the Purdue model (Butler and Williams, 1988; Christensen et al., 1982; Smith and Williams, 1974).

The mass balance for the solid-phase component i is given by

$$\frac{d}{dt}[\alpha_{s_i}\bar{\rho}_s(1-\epsilon)V_c] = \dot{V}_c\alpha_{s_{i_o}}\bar{\rho}_s(1-\epsilon_o) - \dot{V}_c\alpha_{s_i}\bar{\rho}_s(1-\epsilon) + \hat{R}_{s_i}, \tag{3}$$

where α_{s_i} is the mass fraction of solid component i; $\bar{\rho}_s$ is the density of solid material; V_c is the volume of the CSTR which is occupied by wood chips [$V_c = (1-\eta)Ah$]; A is the cross-sectional area of the CSTR (corresponding to the digester); and h is the height of the CSTR. The subscript o denotes inlet flow streams that are the effluent streams of adjacent CSTRs. The density of solid material, $\bar{\rho}_s$, is assumed to be constant. Since the wood chips are assumed to be incompressible, the volumetric flow rate of the chips, $\dot{V}_c$, is constant throughout the digester.

The reaction term is based on the kinetic model developed by Christensen et al. (1982) and is given by

$$\hat{R}_{s_i} = -e_f\left(k_{1,i}\rho_{e_1} + k_{2,i}\rho_{e_1}^{1/2}\rho_{e_3}^{1/2}\right)[\alpha_{s_i}\bar{\rho}_s(1-\epsilon)V_c - \alpha_{s_i}^{\infty}\bar{\rho}_s(1-\epsilon)V_c], \tag{4}$$

where the kinetic rate constants obey Arrhenius temperature dependence:

Table 1. Kinetic Reaction Parameters: Preexponential Factors (for Hardwood and Softwood) and Activation Energies

	1	2	3	4	5
$A_{1,i}$ m^3/kg·min (hardwood)	0.3954	1.457×10^{11}	28.09	7.075	5.8267×10^{3}
$A_{1,i}$ m^3/kg·min (softwood)	0.2809	6.035×10^{10}	6.4509	1.5607	1.0197×10^{4}
$A_{2,i}$ m^3/kg·min (hardwood)	12.49	1.873	124.9	47.86	3.225×10^{16}
$A_{2,i}$ m^3/kg·min (softwood)	9.26	0.489	28.09	10.41	5.7226×10^{16}
$E_{1,i}$ kJ/mol·K	29.3	115	34.7	25.1	73.3
$E_{2,i}$ kJ/mol·K	31.4	37.7	41.9	37.7	167

$$k_{1,i} = A_{1,i}\exp\left(\frac{-E_{1,i}}{RT_c}\right) \quad \text{and} \quad k_{2,i} = A_{2,i}\exp\left(\frac{-E_{2,i}}{RT_c}\right). \tag{5}$$

A free parameter, e_f, is used to adjust the kinetics for different wood species. Since the kinetics of delignification are not known exactly, e_f can be used to "tune" the model behavior to match the observed digester behavior. The preexponential factors ($A_{(1,2),i}$) and the activation energies ($E_{(1,2),i}$) from the earlier Purdue model (Christensen et al., 1982) are converted from English units to metric units and are given in Table 1.

T_c is the temperature of the wood chips and R is the universal gas constant. The mass fraction of solid component i entering the digester, which does not react, is denoted by $\alpha^{\infty}_{s_i}$. The values for the unreactive solid fractions are given in Table 2 and are discussed in detail in Christensen et al. (1982).

Earlier versions of the Purdue model defined the solid-phase concentrations as a mass fraction relative to the total solid mass that entered the digester. In this work, the concentration of solid component i is defined as the mass of component i per chip volume, which is given by

$$\rho_{s_i} = \alpha_{s_i}\bar{\rho}_s(1-\epsilon). \tag{6}$$

The density of the wood substance, $\bar{\rho}_s$, is assumed constant, the mass fraction of the solid-phase component i (α_{s_i}) and the porosity (ϵ) vary with the extent of reaction. Substituting the defined concentration into Eqs. 3 and 4 and applying the differential operator gives the state equations for the solid-phase components (Eq. A1 in the Appendix).

Calculating the chip porosity

The chip porosity is defined as the ratio of the entrapped-liquor volume to the wood-chip volume. Earlier versions of the Purdue model made several simplifying assumptions to calculate the entrapped-liquor volume. The basic idea was to convert the mass of wood to a mass of pulp. The entrapped-liquor volume was the volume of liquor that the pulp mass could hold. In order to calculate this volume, two quantities were assumed, a factor used to convert the wood mass to a pulp mass and a factor used to determine the amount of moisture that pulp could hold.

Table 2. Fraction of Solid Component i, Which Does Not React (or Reacts Very Slowly) During Pulping

	$\alpha^{\infty}_{s_1}$	$\alpha^{\infty}_{s_2}$	$\alpha^{\infty}_{s_3}$	$\alpha^{\infty}_{s_4}$	$\alpha^{\infty}_{s_5}$
Hardwood	0	0	0.65	0.25	0
Softwood	0	0	0.71	0.25	0

In this work, the porosity is directly computed from the solid-phase-component concentrations and the wood-substance density. Summing the masses of the individual solid-phase components and substituting in the concentration definition (Eq. 6) gives the total solid mass per volume of chip:

$$\rho_{s_1}+\rho_{s_2}+\rho_{s_3}+\rho_{s_4}+\rho_{s_5} = \sum_{i=1}^{5}\rho_{s_i} = \sum_{i=1}^{5}\alpha_{s_i}\bar{\rho}_s(1-\epsilon) = \bar{\rho}_s(1-\epsilon)\sum_{i=1}^{5}\alpha_{s_i}. \tag{7}$$

The mass fractions (α_{s_i}) sum to unity, therefore the porosity can be determined by

$$\epsilon = 1 - \frac{\sum_{i=1}^{5}\rho_{s_i}}{\bar{\rho}_s}. \tag{8}$$

Entrapped-liquor-phase component balance

The entrapped liquor is assumed to be homogeneous and to consist of six components; active (or reactive) effective alkali (EA) (e_1); passive (or reacted) EA (e_2); active hydrosulfide (HS) (e_3); passive HS (e_4); dissolved lignin, which is the sum of the dissolved high- and low-reactivity lignin (e_5); and the dissolved carbohydrates, which is the sum of the dissolved cellulose, araboxylan, and galactoglucomman (e_6). The chips are assumed to be completely saturated with water upon entering the digester and devoid of entrapped air.

The reactants from the free liquor diffuse into the entrapped liquor and then react with the solid phase. The reacted material, dissolved solids, and passive reactants then diffuse back into the free liquor. The mass balance for the entrapped-liquor-phase component i is given by

$$\frac{d}{dt}(\alpha_{e_i}\rho_e V_e) = \dot{V}_c\alpha_{e_{i_o}}\rho_{e_o}\epsilon_o - \dot{V}_c\alpha_{e_i}\rho_e\epsilon + k\cdot A_T\alpha_{f_i}\rho_f - k\cdot A_T\alpha_{e_i}\rho_e + \hat{R}_{e_i} + \dot{V}_b\alpha_{f_i}\rho_f. \tag{9}$$

Early Purdue model developers (Christensen et al., 1982; Smith and Williams, 1974) derived a correlation for the mass-diffusion rate ($k\cdot A_T/V_e$) of free-liquor-phase components into the entrapped-liquor phase using measured diffusion coefficient data and formulas for kraft cooked wood chips presented in McKibbins (1960). The correlation for the mass diffussion rate is

$$D = \frac{k \cdot A_T}{V_v} = 6.1321\sqrt{T_c}\, e^{-4{,}870/1.98T_c}\left[\frac{1}{\text{min}}\right]. \quad (10)$$

The entrapped liquor volume is defined as $V_e = \epsilon(1-\eta)Ah$. This correlation assumes that the diffusion of the liquor-phase components are only temperature dependent and that all liquor components diffuse with the same rate. Other diffusion correlations that are dependent on temperature and component concentration have been presented in the literature (Gustafson et al., 1983; Hartler, 1962) and could be easily incorporated into this model.

The reaction term for the entrapped-liquor-phase components is related to the reaction term for the solid-phase components through stoichiometric coefficients. The reaction term for the liquor-phase component i is

$$\hat{R}_{e_i} = \sum_{j=1}^{5} b_{i,j}\hat{R}_{s_j}, \quad (11)$$

where $b_{i,j}$ is the stoichiometric coefficient matrix defined by Eq. A11. The stoichiometric coefficients determine the mass of reactants consumed per mass of solid reacted, and the corresponding values for these coefficients for hardwood and softwood are given in Table 3 (Christensen et al., 1982).

It is assumed that the solids react and dissolve into the entrapped-liquor phase, contributing only mass to the entrapped-liquor phase and not volume. A bulk flow from the free-liquor phase, denoted by $\dot{V}_b$, is assumed to fill the void space that was occupied by the solid material. This flow is dependent on the dissolution of wood substance and is determined from the reaction rate and density of the wood substance as follows:

$$\dot{V}_b = \frac{-\sum_{i=1}^{5} \hat{R}_{s_i}}{\bar{\rho}_s}. \quad (12)$$

The concentration of the entrapped-liquor component i is defined as

$$\rho_{e_i} = \alpha_{e_i}\rho_e. \quad (13)$$

The entrapped-liquor density (ρ_e) is not assumed to be constant, but is implicitly calculated in the state equations for the entrapped-liquor components. Substituting the defined concentration into Eq. 9 and applying the differential operator gives the state equations for the entrapped-liquor-phase components (Eq. A8 in the Appendix).

Table 3. Stoichiometric Coefficients for the Consumption of Effective Alkali and Hydrosulfide

	Softwood	Hardwood	Units
β_{OHL}	0.166	0.21	kg·OH/kg·lignin
β_{OHC}	0.395	0.49	kg·OH/kg·carbohydrate
β_{CSH}	0.039	0.05	kg·HS/kg·lignin

Free-liquor-phase component balance

The free-liquor phase is the bulk liquor surrounding the wood chips and is assumed to consist of the same six components as the entrapped-liquor phase. In the various digester zones the flow of free liquor is either (1) cocurrent or (2) countercurrent with respect to the chip flow. The mass balance for the free-liquor-phase component i is given by

$$\frac{d}{dt}(\alpha_{f_i}\rho_f V_f) = \dot{V}_{f_o}\alpha_{f_{i_o}}\rho_{f_o} - \dot{V}_f\alpha_{f_i}\rho_f + k\cdot A_T\alpha_{e_i}\rho_e - k\cdot A_T\alpha_{f_i}\rho_f - \dot{V}_b\alpha_{f_i}\rho_f \pm \dot{V}_{\text{ext}}\alpha_{f_i,\text{ext}}\rho_{f,\text{ext}}. \quad (14)$$

The flow rate of free liquor entering the CSTR is denoted by $\dot{V}_{f_o}$ and the flow rate of free liquor exiting the CSTR is denoted by $\dot{V}_f$. In general, these values are not equal and further details on their calculation are given below. The volume in the CSTR occupied by the free liquor is $V_f = \eta Ah$.

The external streams that enter and exit the digester in various locations, including the heater outlets and extraction screens, are accounted for at the corresponding CSTR in the lumped approximation. The flow rates and component concentrations in these external streams are $\dot{V}_{\text{ext}}$ and $\alpha_{f_i,\text{ext}}\rho_{f,\text{ext}}$, respectively. The sign of $\dot{V}_{\text{ext}}$ denotes the direction of flow.

The white liquor is assumed to be incompressible and the flow of free liquor entering a CSTR is equal to the flow of free liquor exiting the previous CSTR:

$$\dot{V}_{f_o} = \dot{V}_{f,\text{in},j} = \dot{V}_{f,\text{out},j\pm 1}. \quad (15)$$

The subscript j denotes the CSTR, the positive sign is used for countercurrent chip/liquor flow, and the negative sign is used for cocurrent chip/liquor flow. The flow rate of the free liquor exiting the CSTR is equal to the free-liquor flow rate entering the CSTR minus the bulk flow of free liquor into the entrapped liquor phase plus/minus any external flows:

$$\dot{V}_f = \dot{V}_{f,\text{out},j} = \dot{V}_{f,\text{in},j} - \dot{V}_{b,j} \pm \dot{V}_{\text{ext}}. \quad (16)$$

The concentration of the free-liquor component i is defined as

$$\rho_{f_i} = \alpha_{f_i}\rho_f. \quad (17)$$

The free-liquor density (ρ_f) will vary and is implicitly calculated in the state equations for the free-liquor components. Substituting the defined concentration into Eq. 14 and applying the differential operator gives the state equations for the free-liquor-phase components (Eq. A14 in the Appendix).

The correlation for the mass-diffusion rate given by Eq. 10 is also used to determine the diffusion rate of the entrapped-liquor components into the free-liquor phase. After manipulation of the free-liquor mass-balance equation (Eq. 14), the coefficient for the mass-diffusion rate becomes $(k\cdot A_T)/V_f$. This term is related to the diffusion correlation (Eq. 10) in the following manner:

$$\frac{kA_T}{V_f} = \frac{kA_T}{\eta Ah} = \frac{kA_T}{\epsilon(1-\eta)Ah}\frac{\epsilon(1-\eta)}{\eta}$$

$$= \frac{kA_T}{V_e}\frac{\epsilon(1-\eta)}{\eta} = D\frac{\epsilon(1-\eta)}{\eta}. \quad (18)$$

The factor $\epsilon(1-\eta)/\eta$ relates the component concentrations on the entrapped-liquor volume basis to the component concentrations on the free-liquor volume basis.

Wood-chip and free-liquor energy balances

There are two energy balances derived for each CSTR, one for the wood chips and one for the free liquor. The wood chips consist of two phases, the solid and the entrapped liquor. The time for heat transfer between the two phases is much smaller than other characteristic times in the system, therefore the temperatures of the two phases are assumed to be equal. The energy balances for the wood chips and free liquor, assuming the kinetic and potential energies are negligible, are:

$$\frac{d}{dt}[(Cp_sM_s + Cp_eM_e\epsilon)V_cT_c]$$
$$= \dot{V}_c(Cp_sM_{s_o} + Cp_{e_o}M_{e_o}\epsilon_o)T_{c_o} - \dot{V}_c(Cp_sM_s + Cp_eM_e\epsilon)T_c$$
$$+ \Delta H_R\sum_{i=1}^{5} R_{s_i}V_c + UV_c(T_f - T_c) + \dot{V}_bCp_fM_fT_f + kA_TD_E \quad (19)$$

$$\frac{d}{dt}(Cp_fM_fV_fT_f)$$
$$= \dot{V}_{f_o}Cp_{f_o}M_{f_o}T_{f_o} - \dot{V}_fCp_fM_fT_f + UV_c(T_c - T_f) - \dot{V}_bCp_fM_fT_f$$
$$+ kA_TD_F \pm \dot{V}_{\text{ext}}Cp_{\text{ext}}M_{\text{ext}}T_{\text{ext}}. \quad (20)$$

The total mass in the solid, entrapped-liquor, and free-liquor phases are denoted by M_s, M_e, and M_f, respectively. Due to the fact that the liquor phases consist mainly of water, the mass of water is utilized in the calculation of M_e and M_f. The heat capacity of the solid phase, Cp_s, is assumed to be constant for all of the solid components. The heat capacity of the pure liquor phase (liquor without dissolved solids) is assumed to be constant and equal to the heat capacity of water, Cp_l. Since the entrapped- and free-liquor phases also contain dissolved solids, the following mixing rule is used to determine the heat capacity of the entrapped- and free-liquor phases:

$$Cp_e = Cp_sx_{es} + Cp_lx_{el}$$
$$Cp_f = Cp_sx_{fs} + Cp_lx_{fl}. \quad (21)$$

Here, Cp_e and Cp_f are the heat capacities of the entrapped- and free-liquor phases. The mass fractions of the dissolved solid and liquor components in the entrapped- and free-liquor phases are x_{es}, x_{el}, x_{fs}, and x_{fl}, respectively. This is a common assumption that has been made by other researchers (Smith and Williams, 1974; Michelsen, 1995).

The reactions that occur between the wood substance and the white-liquor components (EA and HS) in the entrapped-liquor phase are exothermic, causing an increase in energy in the wood chips due to reaction. This is modeled using the heat of reaction, ΔH_R, which is the amount of energy released per mass of wood substance reacted. Multiplying this term by the amount of mass reacted, $\sum_{i=1}^{5} R_{s_i}V_c$, determines the increase in wood-chip energy. The heat-transfer coefficient, U, relates the rate of energy transfer due to conduction between the wood chips and the free liquor per degree temperature difference per volume of chip. The value of U used in this work is based on the values determined by earlier Purdue model investigators (Maras et al., 1986). It is assumed that the heat-transfer coefficient is constant throughout the length of the digester. The energy transported with the free-liquor flow into the wood chips, $\dot{V}_b$, is also accounted for in both the wood chips and free-liquor energy balances. This rate of energy transfer is positive for the transfer into the wood chips and negative for the transfer from the free liquor, as reflected in the energy-balance equations.

The net energy that is transported into the chips per volume of diffusing mass is denoted by D_E. This is multiplied by the mass-diffusion-rate coefficient to determine the net energy that is transferred to the chip from mass diffusing between the free- and entrapped-liquor phases. Since some liquor components may be diffusing into the entrapped-liquor phase while others may be diffusing into the free-liquor phase, depending on the component concentration gradient, the correct temperature corresponding to the diffusing component is used. The expression for D_E is

$$D_E = \sum_{i=1}^{4}(\rho_{f_i} - \rho_{e_i})Cp_lT_i + \sum_{i=5}^{6}(\rho_{f_i} - \rho_{e_i})Cp_sT_i, \quad (22)$$

where the temperature T_i is dependent on the component concentration

$$T_i = \begin{cases} T_f & \text{if } \rho_{f_i} > \rho_{e_i} \\ T_c & \text{if } \rho_{f_i} < \rho_{e_i}. \end{cases} \quad (23)$$

The net energy that is transported from the free-liquor phase with the diffusing mass is simply the opposite of the net energy transported to the wood chips:

$$D_F = -D_E. \quad (24)$$

The energy transported to/from the free-liquor phase due to external flows, $\dot{V}_{\text{ext}}$, is also accounted for in the energy balance. Again, the sign of $\dot{V}_{\text{ext}}$ denotes whether the external stream is entering or exiting the CSTR. The total mass and heat capacities of the external streams, M_{ext} and Cp_{ext}, are computed in the same manner as those of the entrapped- and free-liquor phases.

Applying the differential operators in the energy balance equations (Eqs. 19 and 20) and rearranging the terms yield the state equations for the temperatures of the wood chips and the free liquor (Eqs. A18 and A19 in the Appendix).

Table 4. Physical Dimensions of the Digester Model Using the Purdue Model Flow Structure

Parameter	Definition and Value(s)
A	Cross-sectional area of digester (CSTR) (m^2) [17.9854, 17.9854, 17.9854, 17.9854, 17.9854, 17.9854, 17.9854, 17.9854, 17.9854, 17.9854, 17.9854, 17.9854, 18.6793, 19.8650, 19.8650, 19.8650, 21.0871, 21.0871, 21.0871, 21.0871, 21.0871]
h	Height of CSTR (m) [0.6230, 0.6230, 0.6230, 0.6230, 0.6230, 0.5944, 0.5944, 0.5944, 0.5944, 0.4775, 0.4775, 0.4775, 0.6096, 0.6096, 0.6096, 0.5182, 0.5182, 0.5182, 0.7010, 0.7010, 0.7010, 0.7010, 0.7010, 0.7010, 0.7010, 0.7010, 0.7010, 0.7010, 0.7010, 0.7010, 0.7010, 0.4877, 0.4877, 0.4877, 0.6477, 0.6477, 0.6477, 0.6477, 0.6477, 0.6477, 0.6477, 0.6477, 0.3962, 0.7925, 0.3962, 1.1278, 0.6096, 1.0058, 1.0058]

Model outputs

Temperature and concentration profiles can be examined directly from the model states. The sensitivity of these profiles to manipulated inputs, measured and unmeasured disturbances, and model parameters can also be readily examined, which can aid in control-structure selection.

In addition to the model states, other outputs of interest are the Kappa # and the pulp yield. The Kappa #, a measure of the residual lignin concentration in the wood chips, is used as the primary quality-control variable and is defined as

$$\text{Kappa \#} = \frac{(\rho_{s_1} + \rho_{s_2})}{0.00153\left(\sum_{i=1}^{5} \rho_{s_i}\right)}. \tag{25}$$

The Kappa # can be measured using on-line analyzers or laboratory tests; however, its measurement is infrequent and delayed. Secondary measurements, such as temperature and free-liquor concentrations are available at different locations along the digester and can be used in conjunction with a digester model to estimate the value of the Kappa #.

Yield is a measure of the amount of wood substance recovered in comparison with the amount of wood substance fed to the digester and is computed by

$$\text{Yield} = \frac{\sum_{i=1}^{5} \rho_{s_i}(\text{exiting})}{\sum_{i=1}^{5} \rho_{s_i}(\text{entering})}. \tag{26}$$

The control objective for digester operation is to maximize the yield while minimizing the Kappa # variation around the target value. The model developed in this work can be used to find operating conditions to optimize this objective, as well as to compare alternative control structures for Kappa # control.

Simulation Results and Discussion

In order to investigate the impact of the extensions proposed in this article, the extended Purdue model is compared to the earlier version of the Purdue model (Butler and Williams, 1988). The comparison will include both steady-state profiles and dynamic responses to several inputs. The extended Purdue model will also be compared with the Weyerhaeuser digester problem developed by Kayihan et al. (1996). The sensitivity of the extended Purdue model to the heat-transfer coefficient, the diffusion coefficient, and the free liquor to CSTR volume ratio (η profile) is also examined.

Comparison to original Purdue model

The original Purdue model used in the comparison is a single-vessel digester presented by Butler and Williams (1988). There is cocurrent flow of the wood chips and white liquor through both the impregnation and cooking zones. The chips and liquor then flow countercurrently through a wash zone. The digester is shown in Figure 1. The specific physical dimensions, flow structure, and operating parameters of the original Purdue model are found in Butler and Williams (1988). The matching physical dimensions and operating parameters for the extended Purdue model are given in Tables 4 and 5, respectively.

Several steady-state profiles for the original Purdue model and the extended Purdue model are compared. These profiles are the Kappa #, the concentrations of EA, HS and

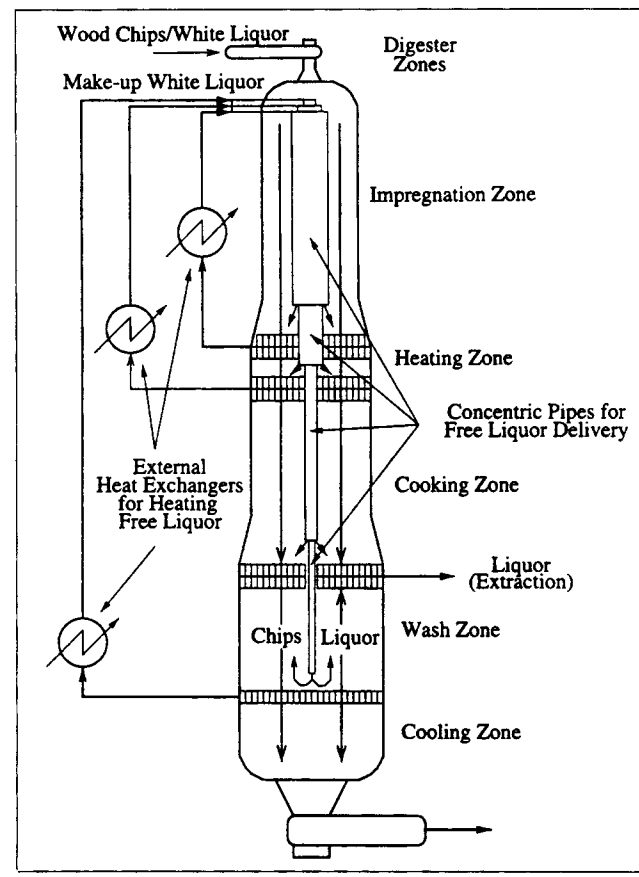

Figure 1. Single-vessel continuous digester.

Table 5. Operating Parameters of the Digester Model Using the Purdue Model Flow Structure

Parameter	Definition and Value(s)
e_f	Reaction rate multiplier [0.9]
$\dot{V}_c$	Entering wood-chip flow rate (m^3/min) [1.3964]
$\dot{V}_f$	Entering white-liquor flow rate (m^3/min) [2.3497]
$\dot{V}_{uphtr}$	Upper heater recirculation flow rate (m^3/min) [7.2728]
T_{uphtr}	Upper heater recirculation temperature (K) [418.83]
$\dot{V}_{lwhtr}$	Lower heater recirculation flow rate (m^3/min) [6.7785]
T_{lwhtr}	Lower heater recirculation temperature (K) [428.64]
$\dot{V}_{\text{quench}}$	Quench recirculation flow rate (m^3/min) [0]
T_{quench}	Quench recirculation temperature (K) [423.15]
$\dot{V}_{\text{wash}}$	Countercurrent wash-zone flow rate (m^3/min) [1.1312]
T_{wash}	Wash-zone heater recirculation temperature (K) [363.40]
$\dot{V}_{w\,\text{circ}}$	Wash-zone recirculation flow rate (m^3/min) [0.2067]
$\dot{V}_{\text{cheat}}$	Cheater flow rate (m^3/min) [0.3514]
$\dot{V}_{\text{filt}}$	Filtrate flow rate (m^3/min) [3.3169]
T_{filt}	Filtrate temperature (K) [360.93]
$T_{c,0}$	Temperature of entering wood chips (K) [395]
$T_{f,0}$	Temperature of entering white liquor (K) [382]
η	Ratio of free liquor phase volume to total CSTR volume (V_f/V) [0.6896, 0.6806, 0.6717, 0.6628, 0.6539, 0.6454, 0.6374, 0.6294, 0.6215, 0.6163, 0.6099, 0.6035, 0.5963, 0.5881, 0.5800, 0.5725, 0.5655, 0.5586, 0.5898, 0.5812, 0.5727, 0.5641, 0.5556, 0.5470, 0.5385, 0.5300, 0.5214, 0.5129, 0.5043, 0.4958, 0.4872, 0.4787, 0.4962, 0.4906, 0.4849, 0.4784, 0.4712, 0.4640, 0.4567, 0.4495, 0.4423, 0.4350, 0.4278, 0.4219, 0.4173, 0.4126, 0.4067, 0.3995, 0.3910, 0.3811]
$\bar{\rho}_s$	Density of solid material (kg/m^3) [1665.9]
$\rho_{s_1,0}$	High reactivity lignin concentration of entering wood chip (kg/m^3) [25.37]
$\rho_{s_2,0}$	Low reactivity lignin concentration of entering wood chip (kg/m^3) [101.49]
$\rho_{s_3,0}$	Cellulose concentration of entering wood chip (kg/m^3) [270.53]
$\rho_{s_4,0}$	Galactoglucomannan concentration of entering wood chip (kg/m^3) [12]
$\rho_{s_5,0}$	Araboxylan concentration of entering wood chip (kg/m^3) [129.03]
$\rho_{e_1,0}$	Active effective alkali concentration in entrapped liquor phase of entering wood chip (kg/m^3) [0]
$\rho_{e_2,0}$	Passive effective alkali concentration in entrapped liquor phase of entering wood chip (kg/m^3) [0]
$\rho_{e_3,0}$	Active hydrosulfide concentration in entrapped liquor phase of entering wood chip (kg/m^3) [0]
$\rho_{e_4,0}$	Passive hydrosulfide concentration in entrapped liquor phase of entering wood chip (kg/m^3) [0]
$\rho_{e_5,0}$	Dissolved lignin concentration in entrapped liquor phase of entering wood chip (kg/m^3) [0]
$\rho_{e_6,0}$	Dissolved carbohydrates concentration in entrapped liquor phase of entering wood chip (kg/m^3) [0]
$\rho_{f_1,0}$	Active effective alkali concentration of entering white liquor (kg/m^3) [78.8]
$\rho_{f_2,0}$	Passive effective alkali concentration of entering white liquor (kg/m^3) [0]
$\rho_{f_3,0}$	Active hydrosulfide concentration of entering white liquor (kg/m^3) [13.3]
$\rho_{f_4,0}$	Passive hydrosulfide concentration of entering white liquor (kg/m^3) [0]
$\rho_{f_5,0}$	Dissolved lignin concentration of entering white liquor (kg/m^3) [59.6]
$\rho_{f_6,0}$	Dissolved carbohydrates concentration of entering white liquor (kg/m^3) [59.6]
$\rho_{f_1,\text{filtrate}}$	Active effective alkali concentration of entering filtrate flow (kg/m^3) [4.8055]
$\rho_{f_2,\text{filtrate}}$	Passive effective alkali concentration of entering filtrate flow (kg/m^3) [0]
$\rho_{f_3,\text{filtrate}}$	Active hydrosulfide concentration of entering filtrate flow (kg/m^3) [0]
$\rho_{f_4,\text{filtrate}}$	Passive hydrosulfide concentration of entering filtrate flow (kg/m^3) [0]
$\rho_{f_5,\text{filtrate}}$	Dissolved lignin concentration of entering filtrate flow (kg/m^3) [45.1159]
$\rho_{f_6,\text{filtrate}}$	Dissolved carbohydrates concentration of entering filtrate flow (kg/m^3) [45.1159]

dissolved solids in both the entrapped- and free-liquor phases, and the temperature of both the wood chips and the free liquor. Using the Kappa #, the solid component concentrations of both the extended and original Purdue models are compared in Figure 2. In both models, the Kappa # increases through the impregnation zone ($z < 0.15$) and then begins to decrease through the cook zone ($0.15 < z < 0.7$). This slight initial increase in Kappa # is due to the quick reaction of araboxylan at lower temperatures. This causes the ratio of lignin to total solids to increase, thus increasing the Kappa #. As temperature increases and the wood chips begin to react, the lignin reacts faster than the carbohydrates through the cook zone, causing the Kappa # to decrease. The chips then enter the countercurrent wash zone ($0.7 < z < 1$) where wash liquor at a lower temperature cools the wood chips. This quenches the reactions between the chips and liquor, giving the constant Kappa # through the wash zone. This cooling is necessary to prevent excessive damage to the cellulose fibers from continued reaction and the mechanical stresses of blowing the pulp from the digester. The Kappa # profiles for the extended and original Purdue models are in close agreement.

The chips are assumed to be initially saturated with water, and the EA and HS concentrations are zero within the entrapped-liquor phase. As the chips and liquor flow through the impregnation zone, the (active) EA and HS diffuse from the free liquor into the entrapped liquor, increasing the EA and HS concentrations in the entrapped liquor and decreasing their concentrations in the free liquor. This is the case for both the extended and the original Purdue models as shown in Figures 3 and 4. Along the cook zone, EA and HS are depleted through reaction. This sustains the concentration gradient and EA and HS continue to diffuse into the entrapped liquor from the free liquor. At the extraction point,

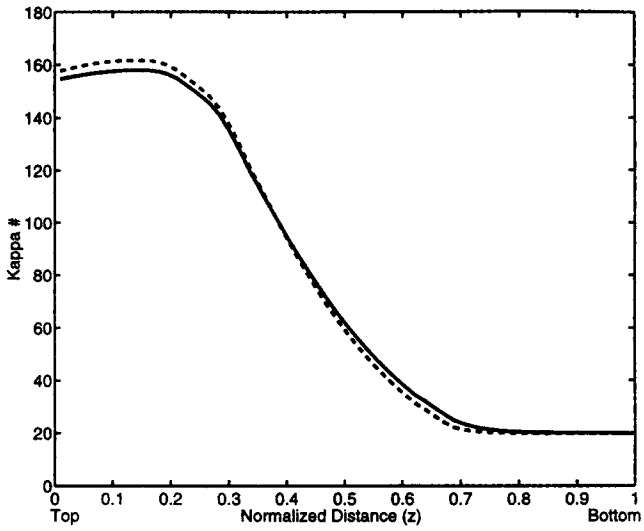

Figure 2. Steady-state Kappa # profiles: extended (solid) vs. original Purdue model (dashed).

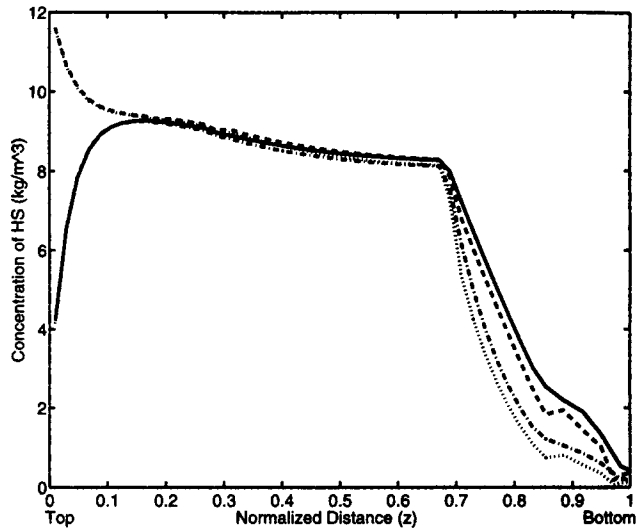

Figure 4. Steady-state profiles of entrapped- and free-liquor (active) HS concentrations: extended vs. original Purdue model.

The entrapped and free liquor of the extended Purdue model are the solid and dashed lines, respectively. The entrapped and free liquor of the original Purdue model are the dash-dot and dotted lines, respectively.

the temperature is reduced and the reactions are quenched. The lower reactant concentrations in the countercurrent wash flow cause the reactants to diffuse back into the free liquor, removing the reactants from the pulp. The comparison between the extended and original Purdue model show that the EA and HS concentration profiles match closely. The EA concentrations in the extended model are slightly higher than those of the original Purdue model, indicating that fewer reactants are consumed during reaction.

The dissolved solids (DS) concentration is a combination of the dissolved lignin and the dissolved carbohydrate concentrations in the liquor phases. The original Purdue model has a flow of black liquor, which is liquor from the extraction point and contains dissolved solids, entering the top of the digester in addition to white liquor. This explains the high concentration of DS at the top of the digester, as shown in Figure 5. The DS concentration in the entrapped liquor quickly increases at the beginning of the impregnation zone ($z < 0.05$) due to diffusion (from the free liquor) and some reaction. As the rate of reactions increase through the cook zone, the DS concentration in the entrapped liquor increases above that of the free liquor. Diffusion from the entrapped liquor increases the free-liquor DS concentration. The DS

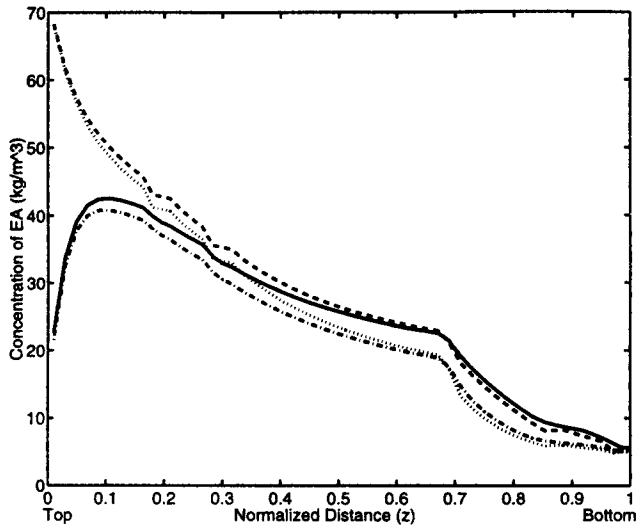

Figure 3. Steady-state profiles of entrapped- and free-liquor (active) EA concentrations: extended vs. original Purdue model.

The entrapped and free liquor of the extended Purdue model are the solid and dashed lines, respectively. The entrapped and free liquor of the original Purdue model are the dash-dot and dotted lines, respectively.

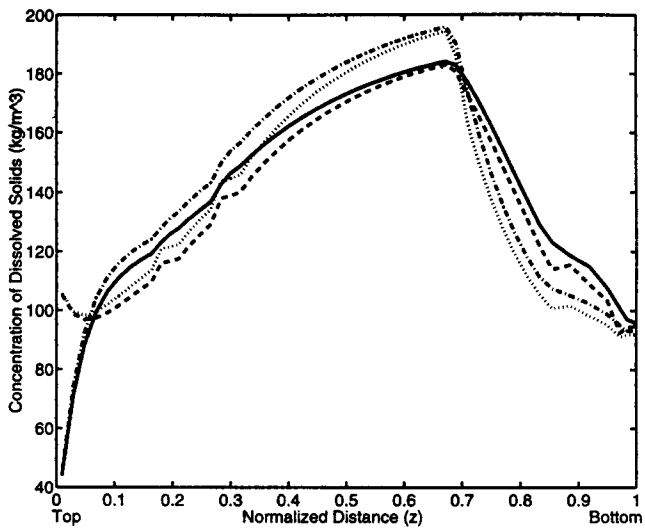

Figure 5. Steady-state profiles of entrapped- and free-liquor DS concentrations: extended vs. original Purdue model.

The entrapped and free liquor of the extended Purdue model are the solid and dashed lines, respectively. The entrapped and free liquor of the original Purdue model are the dash-dot and dotted lines, respectively.

concentration then decreases through the wash zone as the countercurrent wash flow removes the degradation products, which are removed at the extraction screen ($z = 0.7$). The DS concentrations are lower in the extended Purdue model than in the original Purdue model. Overall, the trends between the two models are similar.

The temperature profile of the wood chips and the free liquor are also compared for the two models. The wood-chip temperature, initially ambient, is elevated in a steaming vessel before entering the digester. This is done to remove extractives, such as terpenes, from the chips and to saturate the wood with white liquor, thus reducing buoyance and facilitating reaction. (Again, in this study, the entrapped-liquor phase is assumed to start initially with zero reactants.) The white-liquor temperature is also elevated before entering the digester. The wood chips are heated to reaction temperatures as the chips flow past the upper and lower heaters. Free liquor is circulated through heat exchangers, being introduced to the digester through concentric pipes and extracted at screens just below the entrance of the heated liquor. The effects of the upper and lower heaters are seen in Figure 6 by two discontinuities in the free-liquor temperature. The elevation of the liquor temperature increases the chip temperature, which in turn increases the rate of reaction. The dissolution reactions are exothermic, explaining the increase in temperature through the cook zone. As mentioned before, the temperature is quenched with the countercurrent flow of the wash liquor, slowing the reactions. The temperatures of the wood chips and liquor continue to decrease through the wash zone. The temperature profiles between the extended and original Purdue models match reasonably well.

The differences in the concentration and the temperature profiles between the extended and the original Purdue models are due to the accounting of reacted materials in the extended Purdue model. Since the reacted EA and HS are accounted for in the entrapped- and free-liquor phases, the mass of these phases is increased in the extended Purdue model. This increase in mass allows for more capacity to hold heat. Therefore, the temperatures of the wood chips and the free liquors in the extended Purdue model *do not* increase as much as the temperatures in the original Purdue model through the cooking zone. The reaction rates are slightly slower at these lower temperatures. The slower reaction rates use less EA and HS (giving the higher concentrations) and fewer dissolved solids are formed (giving the lower concentrations). Therefore, the accounting for spent reactants explains the difference seen between the extended and original Purdue models.

The dynamic characteristics of the extended and original Purdue models are also compared. The responses of the Kappa # for the exiting pulp (or blow-line Kappa #) are compared for changes in three inputs: the white-liquor EA concentration, the lower heater temperature, and the white-liquor flow rate. The responses of the blow-line Kappa # to a $\pm 8\%$ step change in the white-liquor EA concentration for both the extended and the original Purdue models are shown in Figure 7. An increase in the white-liquor EA concentration increases the reaction rate, reacting more solids and decreasing the Kappa #. The responses of both models are very similar. The original Purdue model is more sensitive, a 13% larger gain on average, to changes in the white-liquor EA concentration than the extended Purdue model.

The responses of the blow-line Kappa # to a ± 2.8 K step change in the lower heater temperature for both the extended and the original Purdue models are shown in Figure 8. An increase in the cooking temperature also increases the reaction rate. This reacts more solids and decreases the Kappa #. The responses of both models are nearly identical (with the exception of the small offset).

The responses of the blow-line Kappa # to a $\pm 7\%$ step change in the white-liquor flow rate for both the extended and the original Purdue models are shown in Figure 9. An

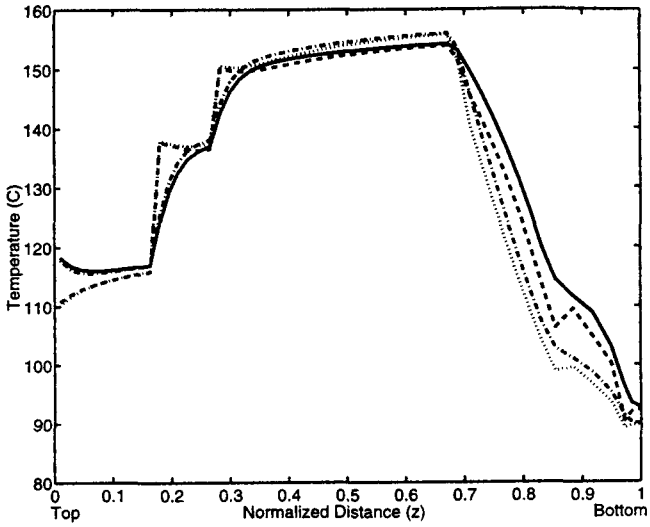

Figure 6. Steady-state profiles of wood-chip and the free-liquor temperatures: extended vs. original Purdue model.

The wood chip and free liquor of the extended Purdue model are the solid and dashed lines, respectively. The wood chip and free liquor of the original Purdue model are the dash-dot and dotted lines, respectively.

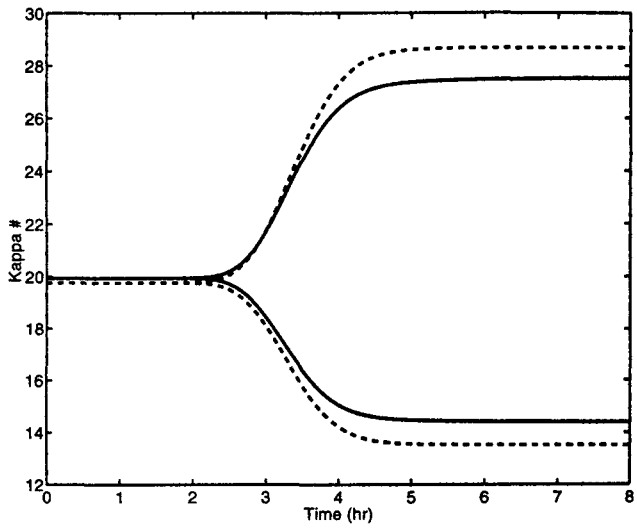

Figure 7. Dynamic responses of the blow-line Kappa #: extended (solid) vs. original Purdue model (dashed) for a $\pm 8\%$ step change in the white-liquor EA concentration.

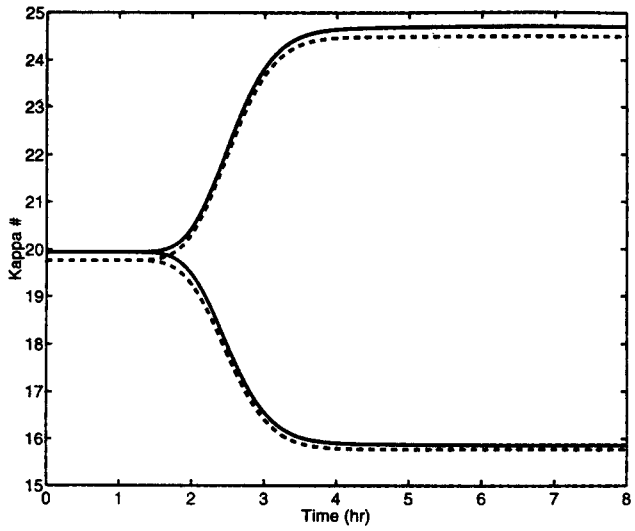

Figure 8. Dynamic responses of the blow-line Kappa #: extended (solid) vs. original Purdue model (dashed) for a ±2.8 K step change in the lower heater temperature.

increase in the white-liquor flow rate increases the amount of reactants entering the digester. This increase helps to maintain a larger concentration gradient of the reactants between the free- and entrapped-liquor phases. Therefore, more reactants diffuse into the entrapped-liquor phase, increasing the reaction rate, reacting more solids, and decreasing the Kappa #. The responses of both models are similar. The original Purdue model shows more sensitivity, an 8% larger gain on average, to the white-liquor flow rate than the extended Purdue model.

Comparison to Weyerhaeuser digester model

The second digester model used to compare with the extended Purdue model is a "simplified" continuous digester model developed by Kayihan et al. (1996) and will be referred to as the Weyerhaeuser digester model (WBD). The WBD is modeled as a two-vessel continuous digester. The first vessel is an impregnation vessel where the wood chips and the white-liquor flow cocurrently. The WBD uses a mixing section plus time delay to model the impregnation vessel. The second vessel is a series of three cooking zones: a regular cocurrent cooking zone; a countercurrent mcc zone; and a countercurrent emcc zone, which will act as both a cooking and washing zone. A dual-vessel digester is shown in Figure 10, and the WBD is shown in Figure 11, which gives the specific physical dimensions and flow structure of the digester. The operating parameters for the WBD are found in (Kayihan et al., 1996). The matching operating parameters for the extended Purdue model are given in Table 6. The $\Delta\kappa\#$, or change in Kappa # from the nominal operating point, are compared between the extended Purdue model and the WBD at three different locations. These locations are at the ends of the cook, mcc, and emcc zones. Step changes in the white-liquor EA concentration, the cooking temperature, and the white-liquor flow rate are considered.

The dynamic responses of $\Delta\kappa\#$ to a ± 5 kg/m^3 step change in the white-liquor EA concentration are shown in Figure 12. For the two-vessel digester structure being considered, the white liquor enters at three separate locations: the beginning of the impregnation zone, and the trim liquors at the bottoms of the mcc and emcc zones. Therefore, step changes in the white-liquor EA concentration have a delayed effect on the Kappa # at the end of the cook zone, but an immediate effect on the Kappa #s at the ends of the mcc and emcc zones. As discussed earlier, increases in the white-liquor EA concentration increase the reaction between the wood components and the white-liquor, and decrease the Kappa #.

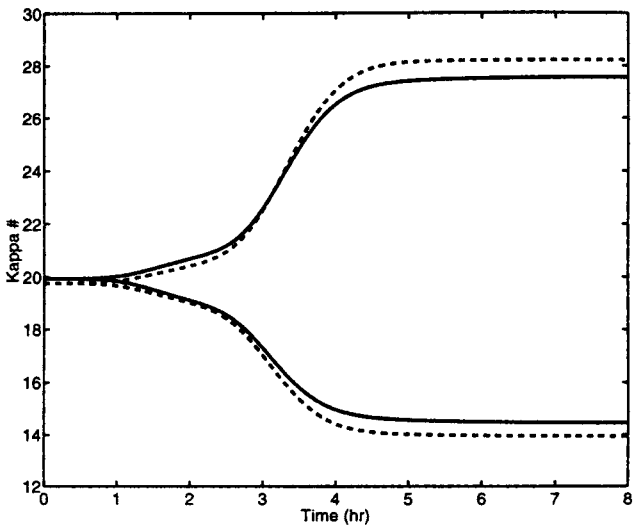

Figure 9. Dynamic responses of the blow-line Kappa #: extended (solid) vs. original Purdue model (dashed) for a ±7% step change in the white-liquor flow rate.

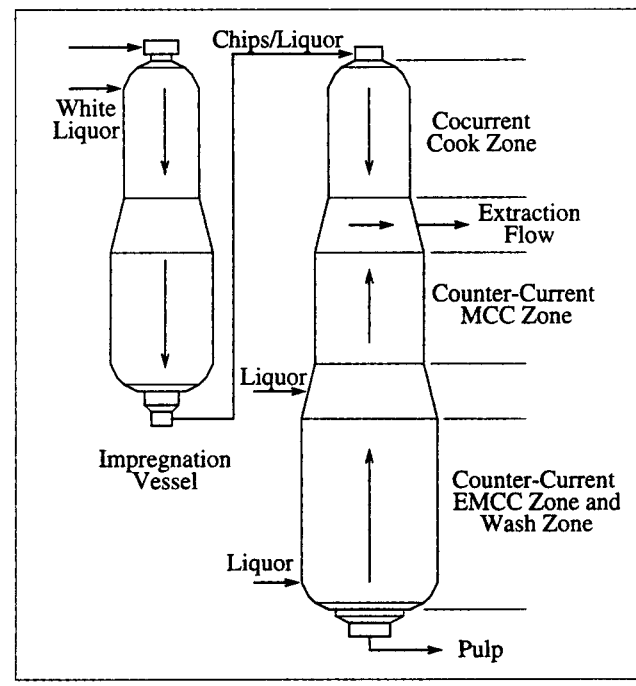

Figure 10. Dual-vessel continuous digester.

The flow structure is similar to that of the Weyerhaeuser digester model.

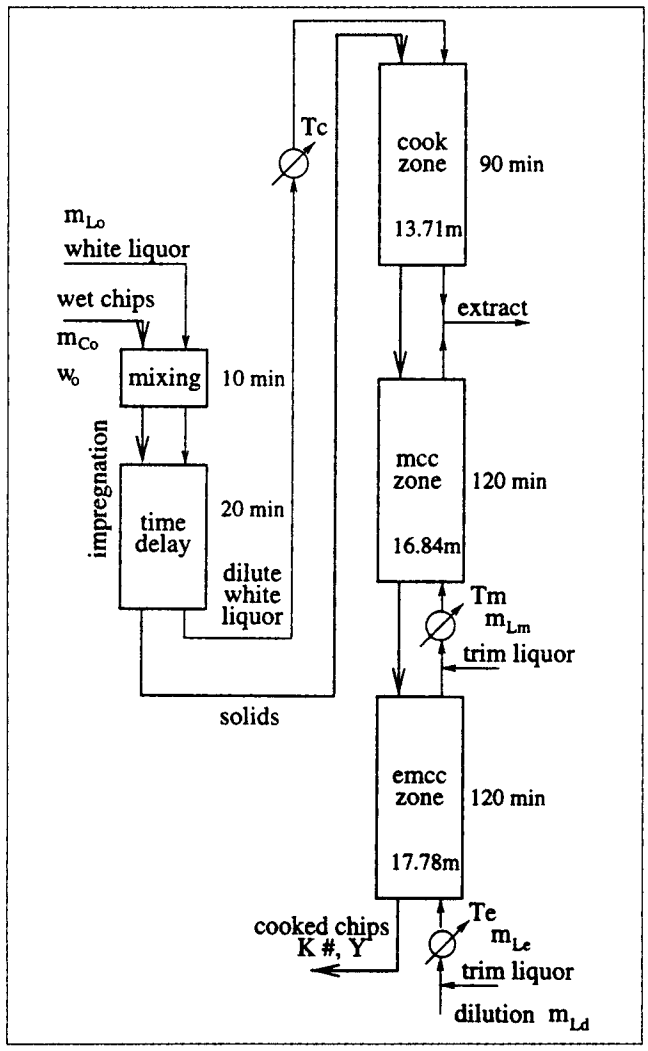

Figure 11. Weyerhaeuser dual-vessel continuous digester.

The dynamic responses of $\Delta\kappa\#$ to a ± 3 K step change in the cooking temperature (T_c) are shown in Figure 13. As seen from the responses, there are significant time delays between the change in the input and the observed change in the output. The WBD is much more sensitive to changes in T_c than the extended Purdue model, as seen by the larger steady-state gains. The responses of both models do exhibit underdamped higher-order behavior.

The dynamic responses of $\Delta\kappa\#$ to a ± 5 kg/min step change in the white-liquor feed flow rate (m_{Lo}) are shown in Figure 14. Since the white liquor is removed at the extraction point just below the cook zone, the immediate effects in the Kappa # due to changes in the white-liquor feed flow rate are seen at the end of the cook zone only. The liquor flow rates and concentrations entering the mcc and emcc zones remain constant, and the delayed effects in the Kappa # seen at the ends of the mcc and emcc zones are the combined effects of reaction in the cook zone and the reactions that occur in these zones. The Kappa # in the extended Purdue model is more sensitive to changes in the white-liquor feed rate than in the WBD.

The extended Purdue model was not validated using real plant data due to the lack of rich, published operational data for the continuous digester, which could exercise the dynamic behavior of fundamental digester models, as noted in Agarwal and Gustafson (1997), for one. Model validity is established through the comparisons with the original Purdue model and the Weyerhaeuser benchmark model, which are accepted by industry as being characteristic of digester operation. The range of behaviors displayed by those models is captured by the extended Purdue model. The differences that do arise between the original and the extended Purdue models are due to the refinements in the fundamental assumptions. These differences could be crucial in applications such as model-based control where the controller is dependent on accurate inferential estimates of the Kappa # obtained from the fundamental model and secondary liquor measurements.

Model parameter sensitivity analysis

A parametric sensitivity analysis for the extended Purdue model is performed using the single-vessel digester configuration. The heat-transfer coefficient, the diffusion coefficients given by correlation Eq. 10, and the free liquor to CSTR volume ratio profile (η) are varied from their base-case values and the steady-state profiles of the model states and Kappa # are compared. For the heat-transfer and diffusion coefficients, the base case is compared to a fivefold increase and a one-fifth decrease in the base-case values. For the η profile, the base case is compared to η profiles, which are scaled $\pm 10\%$ from the base-case values.

The original Purdue model investigators (Christensen et al., 1982; Smith and Williams, 1974) developed the digester model assuming thermal equilibrium between the wood chips and free liquor. Maras et al. (1986) revised the Purdue model by replacing the overall energy balance with separate energy balances for the wood chips and the free liquor. The same kinetic model coefficients were used in the revised model, and, by trial and error, the heat-transfer coefficient was adjusted until the outputs of the revised model matched those of the original model. The heat-transfer coefficient was assumed to be constant throughout the digester, which is also assumed in this work.

The steady-state profiles of the Kappa # and chip temperature for the three different heat-transfer coefficients are compared in Figures 15 and 16, respectively. For the decrease in the heat-transfer coefficient, the resistance to heat conduction is increased, which results in the lower chip temperature profile (from the base case) through the heater and cook zones in Figure 16. This lower temperature during the cooking reduces the amount of reaction, which results in the overall increase in the Kappa # profile in Figure 15. Increasing the heat-transfer coefficient by fivefold does not greatly increase the chip temperature profile from the base case, and has little effect on the Kappa # profile. The value of the heat-transfer coefficient given by Maras et al. (1986) is very close to the limiting case, which is the infinite rate of the heat-conduction case. Therefore, thermal equilibrium between the wood chips and free liquor is a good assumption for these operating conditions and the heat-transfer coefficient value. It is not surprising to find the heat-transfer coefficient to be close to the limiting case, since it was deter-

Table 6. Operating Parameters of the Digester Model Using the Weyerhaeuser Benchmark Model Flow Structure

Parameter	Definition and Value(s)
A	Cross-sectional area of digester (CSTR) (m^2) [1]
e_f	Reaction rate multiplier [0 0.65 0.65 0.65]
h	Heights of the individual zones are given in Figure 11
$\dot{V}_c$	Entering wood-chip flow rate (m^3/min) [0.0667]
$\dot{V}_f$	Entering white-liquor flow rate (m^3/min) [0.0500]
T_{cook}	Cook-zone heater temperature (K) [430]
$\dot{V}_{mcc}$	MCC trim flow rate (m^3/min) [0.0100]
T_{mcc}	MCC heater temperature (K) [410.75]
$\dot{V}_{emcc}$	EMCC trim flow rate (m^3/min) [0.0100]
T_{emcc}	EMCC heater temperature (K) [413.5]
$\dot{V}_{\text{dilution}}$	Dilution flow rate (m^3/min) [0.0700]
$T_{c,0}$	Temperature of entering wood chips (K) [395]
$T_{f,0}$	Temperature of entering white liquor (K) [395]
$\bar{\rho}_s$	Density of solid material (kg/m^3) [1500]
η	Ratio of free liquor phase volume to total CSTR volume (V_f/V) η is a linear relationship from 0.6875 to 0.625 through the IV η is a linear relationship from 0.625 to 0.50 through the cook zone $\eta = 0.525$ and 0.55 through the mcc and emcc zones, respectively
$\rho_{s_1,0}$	High-reactivity lignin concentration of entering wood chip (kg/m^3) [60]
$\rho_{s_2,0}$	Low-reactivity lignin concentration of entering wood chip (kg/m^3) [90]
$\rho_{s_3,0}$	Cellulose concentration of entering wood chip (kg/m^3) [270]
$\rho_{s_4,0}$	Galactoglucomannan concentration of entering wood chip (kg/m^3) [30]
$\rho_{s_5,0}$	Araboxylan concentration of entering wood chip (kg/m^3) [150]
$\rho_{e_1,0}$	Active effective alkali concentration in entrapped liquor phase of entering wood chip (kg/m^3) [0]
$\rho_{e_2,0}$	Passive effective alkali concentration in entrapped liquor phase of entering wood chip (kg/m^3) [0]
$\rho_{e_3,0}$	Active hydrosulfide concentration in entrapped liquor phase of entering wood chip (kg/m^3) [0]
$\rho_{e_4,0}$	Passive hydrosulfide concentration in entrapped liquor phase of entering wood chip (kg/m^3) [0]
$\rho_{e_5,0}$	Dissolved lignin concentration in entrapped liquor phase of entering wood chip (kg/m^3) [0]
$\rho_{e_6,0}$	Dissolved carbohydrates concentration in entrapped liquor phase of entering wood chip (kg/m^3) [0]
$\rho_{f_1,0}$	Active effective alkali concentration of white liquor entering the impregnation vessel, the mcc and emcc trim liquor (kg/m^3) [100]
$\rho_{f_2,0}$	Passive effective alkali concentration of white liquor entering the impregnation vessel, the mcc and emcc trim liquor (kg/m^3) [0]
$\rho_{f_3,0}$	Active hydrosulfide concentration of white liquor entering the impregnation vessel, the mcc and emcc trim liquor (kg/m^3) [30]
$\rho_{f_4,0}$	Passive hydrosulfide concentration of white liquor entering the impregnation vessel, the mcc and emcc trim liquor (kg/m^3) [0]
$\rho_{f_5,0}$	Dissolved lignin concentration of white liquor entering the impregnation vessel, the mcc and emcc trim liquor (kg/m^3) [0]
$\rho_{f_6,0}$	Dissolved carbohydrates concentration of white liquor entering the impregnation vessel, the mcc and emcc trim liquor (kg/m^3) [0]

mined such that the outputs of the model revised by Maras et al. matched those of a model with the thermal-equilibrium assumption. Additional experimental data would be necessary to determine the importance of heat conduction as well as the variation of the heat-transfer coefficient with respect to the extent of reaction and flow regime. If it were determined that heat conduction was insignificant between the two phases compared to other energy-transport mechanisms, the assumption of thermal equilibrium could be used to reduce the two energy-balance equations to one overall energy-balance equation for each CSTR.

The model sensitivity to the rate of mass diffusion between the entrapped- and free-liquor phases is examined by scaling the base-case diffusion-rate coefficients, given in Eq. 10, by five and by one-fifth. Since the digester is approximated with CSTRs, and the wood chips and free liquor in each CSTR are approximated with three homogeneous phases, the effects of wood chip size and geometry on mass diffusion are not explicitly taken into account in the model. An average chip size is implicitly assumed and the resistance to diffusion due to the chip size can be adjusted by scaling the diffusion correlation. For small wood chips, the resistance to diffusion would be small; this effect could be captured with "large" diffusion-rate coefficients that allow faster mass diffusion. For large wood chips, the resistance to diffusion would be large; this effect could be captured with "small" diffusion-rate coefficients that allow slower mass diffusion. To explicitly capture the effects of chip size on the process behavior, the diffusion of mass into the wood chips would need to be modeled, such as the model developed by Gustafson et al. (1983), or through the development of a population balance model such as those described by Ramkrishna (1985). A distribution of chip sizes would be assumed and the effects of this size distribution on the model behavior could be determined as demonstrated by Kayihan (1997).

The steady-state profiles of the Kappa # and the liquor EA concentrations (entrapped and free) for the base case and the scaled diffusion coefficients are compared in Figures 17 and 18, respectively. For the case where the diffusion coefficients are scaled by one-fifth, the rate of mass diffusion between the entrapped- and free-liquor phases is slow, resulting in the large EA concentration gradient shown in Figure

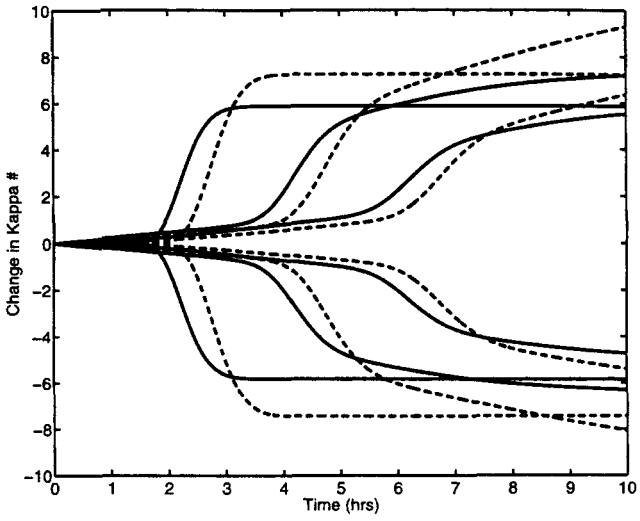

Figure 12. Dynamic responses of $\Delta\kappa$ # located after the cook, mcc, and emcc zones: extended (dashed) vs. Weyerhaeuser digester model (solid) for a ± 5 kg/m^3 step change in the white-liquor EA concentration.

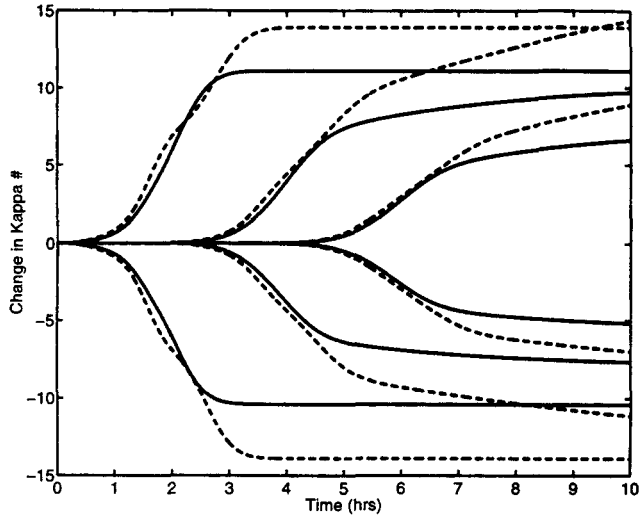

Figure 14. Dynamic responses of $\Delta\kappa$ # located after the cook, mcc, and emcc zones: extended (dashed) vs. Weyerhaeuser digester model (solid) for a ± 5 kg/min step change in the white-liquor flow rate (m_{Lo}).

18. The overall Kappa # profile, shown in Figure 17, is larger for this case, since there is lower reactant concentrations in the entrapped-liquor phase, which results in less reaction. As the diffusion coefficient is increased, the rate of diffusion is increased, which reduces the concentration gradients between the two phases, and the Kappa # profile is lower due to the higher reactant concentrations in the entrapped liquor. The Kappa # profiles for the base case and the increased diffusion coefficients are nearly identical, suggesting that the base case is near a limiting case, which is infinite mass-diffusion rate. The implicit assumption would be that the average wood-chip size is very small, giving little resistance to mass diffusion. The diffusion coefficients could be reduced to simulate a larger average chip size.

As wood chips flow down the digester, the weight of the column causes the individual wood chips to pack closer together, which is referred to as compaction. The compaction profile is modeled as the ratio of the wood chip to CSTR volume. Model sensitivity to the compaction profile is examined by scaling the free liquor to CSTR volume ratio, η, which is the complement of the compaction profile, $(1-\eta)$. The compaction profile is increased along the digester by decreasing the η profile. In this work, the η profile is assumed to be

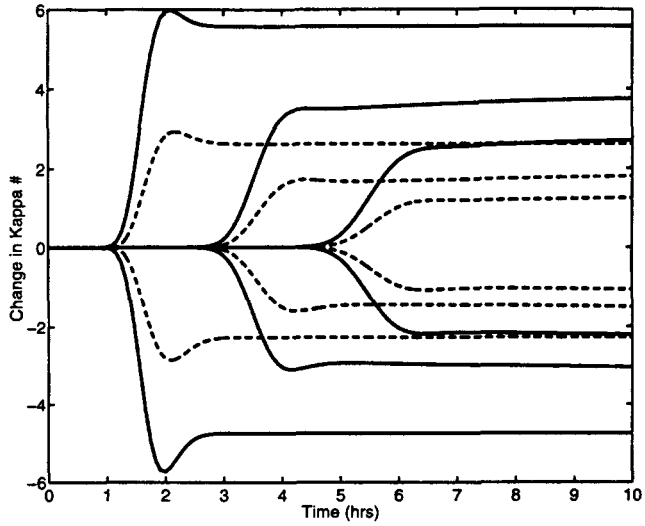

Figure 13. Dynamic responses of $\Delta\kappa$ # located after the cook, mcc, and emcc zones: extended (dashed) vs. Weyerhaeuser digester model (solid) for a ± 3 K step change in the cooking temperature (T_c).

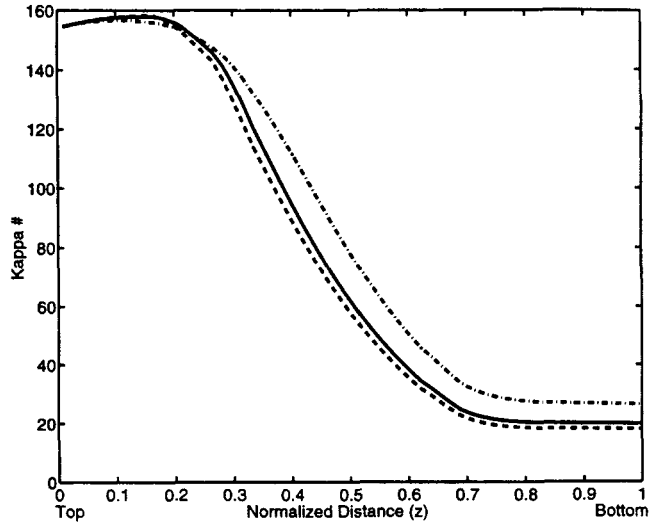

Figure 15. Steady-state Kappa # profiles for varying heat-transfer coefficients.

Base-case heat-transfer coefficient U (solid), 5 times the base case U (dashed), and 1/5 the base case U (dash-dot).

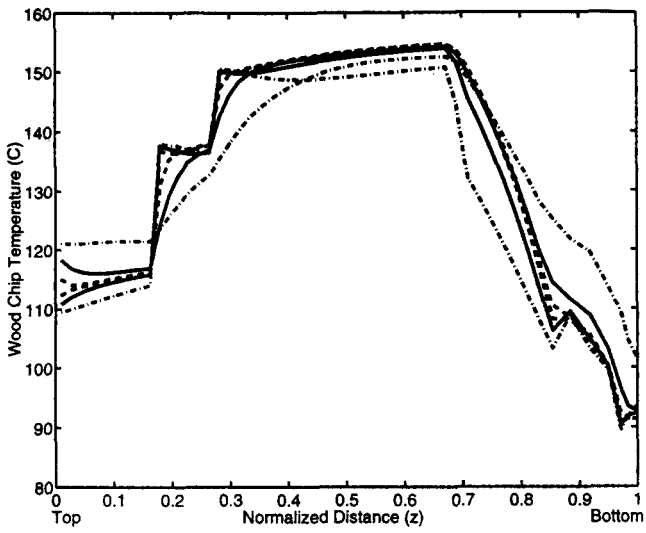

Figure 16. Steady-state chip temperature profiles for varying heat-transfer coefficients.

Base-case heat-transfer coefficient U (solid), 5 times the base case U (dashed), and 1/5 the base case U (dash-dot).

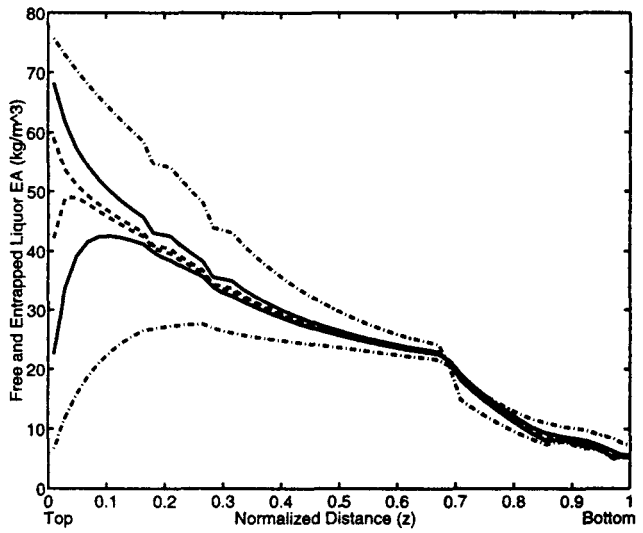

Figure 18. Steady-state free- and entrapped-liquor EA profiles for varying diffusion coefficients.

Base-case diffusions coefficient D_j given by Eq. 10 (solid), $5D_j$ (dashed), and $D_j/5$ (dash-dot).

known. Reasonable values can be assumed and the profile can be adjusted to "tune" the model behavior to match the observed behavior of an actual digester. However, it is physically impossible to know the exact (possibly time varying) η profile in an actual digester.

The base-case η profile, given in Table 5, is scaled by $\pm 10\%$ and the steady-state profiles of Kappa # for the different η profiles are compared in Figure 19. The Kappa # profile is decreased for the 10% decrease in η and is increased for the 10% increase in η. The 10% decrease in the η profile is a 10% increase in the compaction profile which, in turn, is a 10% increase in the wood-chip volume in the digester. Since the volumetric flow rate of wood chips is constant in this study, the increase in the volume occupied by the wood chips translates to an increased residence time, thus allowing the wood chips to "cook" for a longer time. Therefore, the Kappa # profile is lower for the 10% decrease in η. As the η profile is increased, the residence time for the wood chips is decreased and the Kappa # profile increases. The positive and negative scaling of η give similar bilateral variations in the Kappa # profiles, thus making the η a versatile tuning parameter to adjust the Kappa # profile to match observed digester behavior.

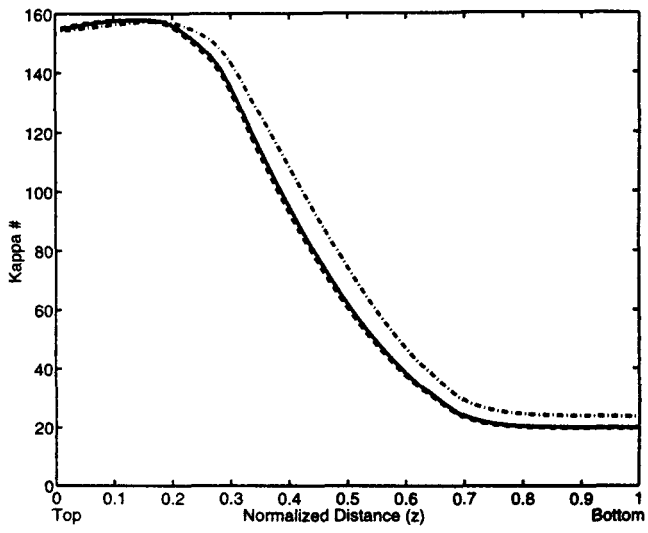

Figure 17. Steady-state Kappa # profiles for varying diffusion coefficients.

Base-case diffusions coefficient D_j given by Eq. 10 (solid), $5D_j$ (dashed), and $D_j/5$ (dash-dot).

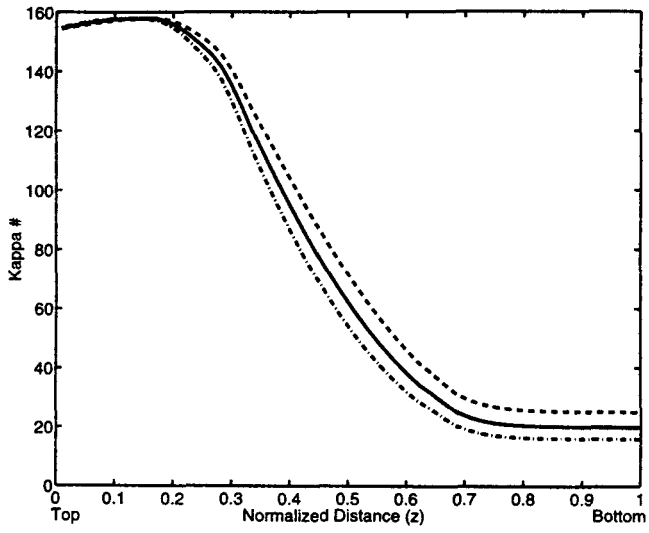

Figure 19. Steady-state Kappa # profiles for varying the ratio of free-liquor volume to total CSTR volume (η).

Base-case η given in the Appendix (solid), 10% increase in η (dashed), and a 10% decrease in η (dash-dot).

Conclusions

The digester model presented in this work is an extension of the well-known Purdue digester model. This model can be used for simulation and control studies, optimization of operating parameters, and design analysis. It captures the important physical behavior of the digester in a direct implementation form.

The extensions proposed in this work allow a relaxation of the assumptions of an already proven, industrially accepted, digester model. The approach to modeling is similar to the original Purdue model, the digester is approximated with a series of CSTRs, each CSTR consisting of three phases. By defining the solids concentrations on a mass per chip volume basis and defining the compaction and porosity as volume fractions of the CSTR and wood chip, respectively, several assumptions used in the original model were removed. In particular, the extended model calculates chip porosity and liquor densities as functions of the wood reaction. These types of improvements in the model foundation will be necessary for the next generation of interesting digester control studies, such as optimal transition control (which include feedstock swings), in addition to unmeasured disturbance rejection.

The steady-state profiles and dynamic responses of the extended Purdue model closely match those of the original Purdue model. The differences can be attributed to the accounting of reacted material in the extended version. This increases the capacity to hold heat (more than the original Purdue model), which lowers the temperature profiles of the wood chips and liquor in the extended version. The lower temperatures reduce the amount of reaction and use fewer reactants than predicted by the original Purdue model. These differences could be crucial in applications such as optimization and control. True model validation will only be realized by the availability of rich dynamic data for the continuous digester. The extended model's ability to extrapolate over a wider range of operating conditions would be expected due to the refinements in the model.

The extended model is "tuned" such that its dynamic behaviors compare favorably to those of the Weyerhaeuser benchmark digester model. The model is versatile in that it can be easily configured for different digester flow structures and capture the essential characteristics of the pulping process.

The parametric sensitivity of the extended Purdue model to the heat-transfer coefficient, the diffusion coefficients, and the free liquor to CSTR volume ratio (η) profile is also examined. It is shown that the base-case heat-transfer coefficient and the diffusion coefficients values are very near the limiting cases, which is infinite rate heat transfer and mass diffusion, respectively. The η profile could be varied along the length of the digester to adjust the Kappa # profile, making it an effective model "tuning" parameter.

Due to the expensive nature of conducting experiments on actual plant units, it is often advantageous to first conduct virtual experiments on a simulation model. Using this continuous digester model, engineers and researchers can perform identification and control structure selection experiments as well as analyze various types of controllers. The model itself could be incorporated into a model-based controller such as model-predictive control (MPC). The model can also be used in conjunction with optimization packages to determine optimal operating parameters (Sidrak, 1995). An objective would be to determine the operating conditions that minimize waste and energy while maximizing yield for various target Kappa #s. Another advantage of the easy implementation is the ability to reconfigure the digester quickly for different flow structures. This allows for the analysis of different digester designs to determine if better pulp quality could be achieved with more control-relevant digester designs.

Acknowledgments

P.A.W. and F.J.D. gratefully acknowledge funding from the Weyerhaeuser Company through CIPAC at Purdue University and NSF CTS 9257059. The authors also thank Marc S. Gelormino of Weyerhaeuser Company for his insightful discussion of digester modeling and for providing the Weyerhaeuser Benchmark Digester simulation model.

Notation

D_F = energy transported with diffusion into free liquor, kJ/m^3
$k \cdot A_T$ = diffusion coefficient, m^3/min
$k_{(1,2),i}$ = reaction-rate constant, m^3/min·kg
R_{s_i} = reaction rate of solid component i, kg/min·m^3
T_{ext} = temperature of external stream, K
T_f = temperature of free liquor, K
y = Kappa #
α_{e_i} = mass fraction of entrapped-liquor component i, kg/kg
α_{f_i} = mass fraction of free-liquor component i, kg/kg
ρ_{e_1} = active effective alkali concentration in entrapped-liquor phase, kg/m^3
ρ_{e_2} = passive effective alkali concentration in entrapped-liquor phase, kg/m^3
ρ_{e_3} = active hydrosulfide concentration in entrapped-liquor phase, kg/m^3
ρ_{e_4} = passive hydrosulfide concentration in entrapped-liquor phase, kg/m^3
ρ_{e_5} = water concentration in entrapped-liquor phase, kg/m^3
ρ_{e_6} = dissolved lignin concentration in entrapped-liquor phase, kg/m^3
ρ_{e_7} = dissolved carbohydrates concentration in entrapped-liquor phase,kg/m^3
ρ_{f_1} = active effective alkali concentration in free-liquor phase, kg/m^3
ρ_{f_2} = passive effective alkali concentration in free-liquor phase, kg/m^3
ρ_{f_3} = active hydrosulfide concentration in free-liquor phase, kg/m^3
ρ_{f_4} = passive hydrosulfide concentration in free-liquor phase, kg/m^3
ρ_{f_5} = water concentration in free-liquor phase, kg/m^3
ρ_{f_6} = dissolved lignin concentration in free-liquor phase, kg/m^3
ρ_{f_7} = dissolved carbohydrates concentration in free-liquor phase, kg/m^3

Literature Cited

Agarwal, N., and R. Gustafson, "A Contribution to the Modeling of Kraft Pulping," *Can. J. Chem. Eng.*, **75**, 8 (1997).

Butler, A. C., and T. J. Williams, "A Description and User's Guide for the Purdue Kamyr Digester Model," Tech. Rep. 152, Purdue Univ., PLAIC, West Lafayette, IN (1988).

Christensen, T., L. F. Albright, and T. J. Williams, "A Mathematical Model of the Kraft Pulping Process," Tech. Rep. 129, Purdue Univ., PLAIC, West Lafayette, IN (1982).

Gustafson, R. R., C. A. Sleicher, W. T. McKean, and B. A. Finlayson, "Theoretical Model of the Kraft Pulping Process," *Ind. Eng. Chem. Process Des. Dev.*, **22**(1), 87 (1983).

Härkonen, E. J., "A Mathematical Model for Two-Phase Flow in a Continuous Digester," *TAPPI J.*, **70**, 122 (1987).

Hartler, N., "Penetrerings-Och Diffusionsforhålandena vid Sufatkoket," *Pap. och Trä*, **44**(7), 365 (1962).
Hatton, J., "Development of Yield Prediction Equations in Kraft Pulping," *TAPPI J.*, **56**, 97 (1973).
Hatton, J., "The Potential of Process Control in Kraft Pulping of Hardwoods Relative to Softwoods," *TAPPI J.*, **59**, 48 (1976).
Jiménez, G., R. Gustafson, and W. McKean, "Modelling Incomplete Penetration of Kraft Pulping Liquor," *J. Pulp Pap. Sci.*, **15**(3), J110 (1989).
Kayihan, F., "Model-based Management of Continuous Digesters to Minimize Kappa Number Variability," AIChE Meeting, Los Angeles (1997).
Kayihan, F., M. Gelormino, E. Hanczyc, F. Doyle, III, and Y. Arkun, "A Kamyr Continuous Digester Model for Identification and Controller Design," *Proc. IFAC World Cong.*, San Francisco, p. 37 (1996).
Lee, J., and A. Datta, "Nonlinear Inferential Control of Pulp Digesters," *AIChE J.*, **40**(1), 50 (1994).
Maras, J. T., G. B. Stark, L. F. Albright, and T. J. Williams, "Modelling and Simulation of a Kamyr Digester," Tech. Rep. 150, Purdue Laboratory for Applied Industrial Control, Purdue Univ., West Lafayette, IN (1986).
McKibbins, S. W., "Application of Diffusion Theory to the Washing of Kraft Cooked Wood Chips," *TAPPI J.*, **43**, 801 (1960).
Michelsen, F. A., "A Dynamic Mechanistic Model and Model-Based Analysis of a Continuous Kamyr Digester," PhD Thesis, Univ. of Trondheim, Norway (1995).
Olm, L., and G. Tistad, "Kinetics of the Initial Stage of Kraft Pulping," *Sven. Papperstidn.*, **82**(15), 458 (1979).
Paulonis, M. A., and A. Krishnagopalan, "Kappa Number and Overall Yield Calculation Based on Digester Liquor Analysis," *TAPPI J.*, **71**, 185 (1988).
Ramkrishna, D., "The Status of Population Balances," *Rev. Chem. Eng.*, **3**(1), 49 (1985).
Sidrak, Y., "Model-based Optimization of Kamyr Digester Operation," *TAPPI J.*, **78**, 93 (1995).
Smith, C. C., and T. J. Williams, "Mathematical Modeling, Simulation and Control of the Operation of Kamyr Continuous Digester for Kraft Process," Tech. Rep. 64, Purdue Univ., PLAIC, West Lafayette, IN (1974).
Vanchinathan, S., and G. Krishnagopalan, "Dynamic Modeling of Kraft Pulping of Southern Pine Based on On-line Liquor Analysis," *TAPPI J.*, **80**, 123 (1997).
Vroom, K. E., "The 'H' Factor: A Means of Expressing Cooking Times and Temperatures as a Single Variable," *Pulp. Pap. Mag. Can.*, Convention Issue (1957).

Appendix

State equations for the solid-phase components

$$\dot{\rho}_{s_i,j} = \frac{\dot{V}_c}{V_{c,j}}(\rho_{s_i,j-1} - \rho_{s_i,j}) + R_{s_i,j} \qquad i = 1, \ldots, 5 \quad \text{(A1)}$$

$$R_{s_i,j} = -e_{f,j}\left(k_{1,i}\rho_{e_1,j} + k_{2,i}\rho_{e_1,j}^{1/2}\rho_{e_3,j}^{1/2}\right)(\rho_{s_i,j} - \rho_{s_i}^{\infty}) \quad \text{(A2)}$$

$$k_{1,i,j} = A_{1,i}\exp\left(\frac{-E_{1,i}}{RT_{c,j}}\right) \quad \text{(A3)}$$

$$k_{2,i,j} = A_{2,i}\exp\left(\frac{-E_{2,i}}{RT_{c,j}}\right) \quad \text{(A4)}$$

$$V_{c,j} = (1-\eta_j)A_j h_j. \quad \text{(A5)}$$

The subscript j denotes the CSTR in the series of CSTRs. The universal gas constant is $R = 0.0083144$ kJ/mol·K.

Calculating porosity and change in porosity

$$\epsilon_j = 1 - \frac{\sum_{i=1}^{5}\rho_{s_i,j}}{\bar{\rho}_s} \quad \text{(A6)}$$

$$\dot{\epsilon}_j = -\frac{\sum_{i=1}^{5}\dot{\rho}_{s_i,j}}{\bar{\rho}_s}. \quad \text{(A7)}$$

State Equations for the Entrapped-Liquor-Phase Components

$$\dot{\rho}_{e_i,j} = -\frac{\rho_{e_i,j}}{\epsilon_j}\dot{\epsilon}_j + \frac{\dot{V}_c}{V_{e,j}}(\rho_{e_i,j-1}\epsilon_{j-1} - \rho_{e_i,j}\epsilon_j) + D_j(\rho_{f_i,j} - \rho_{e_i,j}) + \frac{R_{e_i,j}}{\epsilon_j} + \frac{\dot{V}_{b,j}\rho_{f_i,j}}{V_{e,j}} \qquad i = 1, \ldots, 6 \quad \text{(A8)}$$

$$R_{e_i,j} = \sum_{l=1}^{5} b_{i,l}R_{s_l,j} \qquad i = 1, \ldots, 6 \quad \text{(A9)}$$

$$V_{e,j} = \epsilon_j(1-\eta_j)A_j h_j \quad \text{(A10)}$$

$$b = \begin{bmatrix} \beta_{OHL} - \frac{1}{2}\beta_{HSL} & \beta_{OHL} - \frac{1}{2}\beta_{HSL} & \beta_{OHC} & \beta_{OHC} & \beta_{OHC} \\ -\left(\beta_{OHL} - \frac{1}{2}\beta_{HSL}\right) & -\left(\beta_{OHL} - \frac{1}{2}\beta_{HSL}\right) & -\beta_{OHC} & -\beta_{OHC} & -\beta_{OHC} \\ \frac{1}{2}\beta_{HSL} & \frac{1}{2}\beta_{HSL} & 0 & 0 & 0 \\ -\frac{1}{2}\beta_{HSL} & -\frac{1}{2}\beta_{HSL} & 0 & 0 & 0 \\ -1 & -1 & 0 & 0 & 0 \\ 0 & 0 & -1 & -1 & -1 \end{bmatrix} \quad \text{(A11)}$$

$$\beta_{\mathrm{OHL}} = \frac{\text{mass of OH consumed}}{\text{mass of lignin reacted}}\left[\frac{m_{e_1}}{m_{s_1}+m_{s_2}}\right]$$

$$\beta_{\mathrm{HSL}} = \frac{\text{mass of HS consumed}}{\text{mass of lignin reacted}}\left[\frac{m_{e_3}}{m_{s_1}+m_{s_2}}\right]$$

$$\beta_{\mathrm{OHC}} = \frac{\text{mass of OH consumed}}{\text{mass of carbohydrate reacted}}\left[\frac{m_{e_1}}{m_{s_3}+m_{s_4}+m_{s_5}}\right].$$

The temperature-dependent diffusion correlation:

$$D_j = 6.1321\sqrt{T_{c,j}}\,e^{-4.870/1.98T_{c,j}}. \tag{A12}$$

The bulk flow of free liquor into the entrapped liquor phase to fill the void created by the reaction of the solid-phase material:

$$\dot{V}_{b,j} = \frac{-\sum_{i=1}^{5}\hat{R}_{s_i,j}}{\bar{\rho}_s}. \tag{A13}$$

State equations for the free-liquor-phase components

$$\dot{\rho}_{f_i,j} = \frac{\dot{V}_{f,\mathrm{in},j}}{V_{f,j}}\rho_{f_i,j\pm1} - \frac{\dot{V}_{f,\mathrm{out},j}}{V_{f,j}}\rho_{f_i,j} + D_j\frac{\epsilon_j(1-\eta_j)}{\eta_j}(\rho_{e_i,j}-\rho_{f_i,j}) + \frac{\dot{V}_{b,j}}{V_{f,j}}\rho_{f_i,j} \pm \frac{\dot{V}_{\mathrm{ext}}}{V_{f,j}}\rho_{f_i,\mathrm{ext}}$$

$$i = 1, \ldots, 6 \tag{A14}$$

$$V_{f,j} = \eta_j A_j h_j \tag{A15}$$

$$\dot{V}_{f,\mathrm{in},j} = \dot{V}_{f,\mathrm{out},j\pm1} \tag{A16}$$

$$\dot{V}_{f,\mathrm{out},j} = \dot{V}_{f,\mathrm{in},j} - \dot{V}_{b,j} \pm \dot{V}_{\mathrm{ext}}. \tag{A17}$$

State equation for the wood-chip temperature

$$\dot{T}_{c,j} = -\frac{\left(Cp_s\dot{M}_{s,j} + Cp_{e,j}M_{e,j}\dot{\epsilon}_j + Cp_{e,j}\dot{M}_{e,j}\epsilon_j\right)T_{c,j}}{Cp_sM_{s,j} + Cp_{e,j}M_{e,j}\epsilon_j} + \frac{\dot{V}_c}{V_c}\left(\frac{Cp_sM_{s,j-1} + Cp_{e,j-1}M_{e,j-1}\epsilon_{j-1}}{Cp_sM_{s,j} + Cp_{e,j}M_{e,j}\epsilon_j}T_{c,j-1} - T_{c,j}\right) + \frac{\Delta H_R\sum_{i=1}^{5}R_{s_i,j}}{Cp_sM_{s,j} + Cp_{e,j}M_{e,j}\epsilon_j} + \frac{U}{Cp_sM_{s,j} + Cp_{e,j}M_{e,j}\epsilon_j}(T_{f,j} - T_{c,j}) + \frac{\dot{V}_{b,j}}{V_c} \times \frac{Cp_{f,j}M_{f,j}T_{f,j}}{Cp_sM_{s,j} + Cp_{e,j}M_{e,j}\epsilon_j} + \frac{D_jD_{E,j}}{Cp_sM_{s,j} + Cp_{e,j}M_{e,j}\epsilon_j} \tag{A18}$$

$$\dot{T}_{f,j} = -\frac{\dot{M}_{f,j}T_{f,j}}{M_{f,j}} + \frac{\dot{V}_{f,j\pm1}}{V_f}\frac{Cp_{f,j\pm1}M_{f,j\pm1}}{Cp_{f,j}M_{f,j}}T_{f,j\pm1} - \frac{\dot{V}_{f,j}}{V_{f,j}}T_{f,j} + \frac{U}{Cp_{f,j}M_{f,j}}\frac{(1-\eta)}{\eta}(T_{c,j}-T_{f,j}) - \frac{\dot{V}_{b,j}}{V_{f,j}}T_{f,j} + \frac{D_jD_{F,j}}{Cp_{f,j}M_{f,j}}\frac{(1-\eta)}{\eta} \pm \frac{Cp_{f,\mathrm{ext}}M_{f,\mathrm{ext}}}{Cp_{f,j}M_{f,j}}\frac{\dot{V}_{\mathrm{ext}}}{V_{f,j}}T_{\mathrm{ext}}. \tag{A19}$$

$$M_{s,j} = \sum_{i=1}^{5}\rho_{s_i,j} \tag{A20}$$

$$M_{e,j} = M_{el,j} + M_{es,j} \tag{A21}$$

$$M_{f,j} = M_{fl,j} + M_{fs,j} \tag{A22}$$

$$M_{el,j} = \sum_{i=1}^{4}\rho_{e_i,j} + \rho_{\mathrm{water}} \tag{A23}$$

$$M_{es,j} = \sum_{i=5}^{6}\rho_{e_i,j} \tag{A24}$$

$$M_{fl,j} = \sum_{i=1}^{4}\rho_{f_i,j} + \rho_{\mathrm{water}} \tag{A25}$$

$$M_{fs,j} = \sum_{i=5}^{6}\rho_{f_i,j}. \tag{A26}$$

$$Cp_{e,j} = Cp_l\frac{M_{el,j}}{M_{e,j}} + Cp_s\frac{M_{es,j}}{M_{e,j}} \tag{A27}$$

$$Cp_{f,j} = Cp_l\frac{M_{fl,j}}{M_{f,j}} + Cp_s\frac{M_{fs,j}}{M_{f,j}}. \tag{A28}$$

The heat capacities of the wood substance and the liquor are $Cp_s = 1.47$ kJ/kg·K and $Cp_l = 4.19$ kJ/kg·K. The heat of reaction is $\Delta H_R = -581$ kJ/kg, and the heat-transfer coefficient is $U = 827$ kJ/min·K·m^3. The energy transported with mass diffusing from the free to the entrapped liquor phases:

$$D_{E,j} = \sum_{i=1}^{4}(\rho_{f_i,j} - \rho_{e_i,j})Cp_lT_{i,j} + \sum_{i=5}^{6}(\rho_{f_i,j} - \rho_{e_i,j})Cp_sT_{i,j}, \tag{A29}$$

where

$$T_{i,j} = \begin{cases} T_{f,j} & \text{if } \rho_{f_i,j} > \rho_{e_i,j} \\ T_{c,j} & \text{if } \rho_{f_i,j} < \rho_{e_i,j}. \end{cases} \tag{A30}$$

The energy transported with mass diffusing from the entrapped to the free-liquor phases:

$$D_{F,j} = -D_{E,j}. \tag{A31}$$

Manuscript received Apr. 25, 1997, and revision received July 31, 1997.